



## Bending of Exponentially Graded Plates using new HSDT

Bathini Sidda Reddy<sup>a,\*</sup>, Ch. Ravikiran<sup>b</sup> and K. Vijaya Kumar Reddy<sup>c</sup>

<sup>a</sup>Department of Mech. Engg., Rajeev Gandhi Memorial College of Engg., and Tech., Nandyal, Kurnool (Dt), Andhra Pradesh, India-518 501. Fax:08514 275203

<sup>b</sup>Department of Mech. Engg., MLR Institute of Technology, Telangana, India-500043

<sup>c</sup>Department of Mech. Engg., JNTUH, Telangana, India-500085

---

### Article info:

Received: 00/00/2000

Accepted: 00/00/2018

Online: 00/00/2018

### Keywords:

EGM Plate,  
Bending Analysis,  
Navier's Method,  
Thermal and mechanical  
loading.  
Novel Theory

### Abstract

The present paper considers the devise and development of a novel theory to examine the flexure analysis of exponentially graded plates exposed to thermal and mechanical loads. The properties such as Elastic moduli and thermal moduli are assumed to vary exponentially along the thickness by keeping the poisons ratio as constant. This theory fulfils the nullity conditions on the upper side and lower side of the exponentially graded plates for transverse shear stress. The Hamilton's principle has been used to derive the equation of motion. The present theory numerical results are assessed with three-dimensional elasticity solutions and the results of other authors available in the literature. The influence of thermo mechanical loads and thickness ratios and aspect ratios on the bending response of exponentially graded plates are studied in detail. The analytical formulations and solutions presented herein could provide engineers with the potential for the design and development of exponentially graded plates for advanced engineering applications.

### Keywords

EGM plate, bending analysis, Navier's Method, Thermal and Mechanical loading, Novel theory.

---

### Nomenclature

a	Length of EGM plate
b	Width of EGM plate
h	Thickness of the plate
P (z)	Property of the EGM plate
u,v	Inplane displacement in x and y- directions
w	Transverse displacemet
$\epsilon$	Strain

## 1. Introduction

Functionally graded materials (FGMs) are advanced materials whose properties are assorted in a predetermined manner to enhance the overall structural functioning. Nowadays FGMs are substitute materials in several structural applications used in situations where the operating conditions are severe.

---

\*Corresponding author

Email address: sidhareddy\_548@rediffmail.com

Typically, FGMs are fabricated by mixing two different material phases with continuous composition gradation. Such gradation gives smooth variation in material properties. Most plate structures are normally exposed to thermal and mechanical load. In fact, the FGM plates and shells are used to resist high temperature environments. Conversely, due to the heterogeneity and wide spread utilization of FGMs in structural members require the necessity to develop simple and precise theoretical models to understand the behaviour of the structures.

In the past, many authors have paid great effort in modelling of the composite/sandwich plates and introduced various plate theories to study the FGMs behaviour. Reddy and Chin [1], Zenkour [2-4], Kant and Co-workers [5-9], Kadkhodayan[10], Matsunaga [11-12], Xiang [13], Sidda Reddy et al. [14-15] and Suresh Kumar et al. [16]. Used third order displacement terms in the thickness direction to develop the higher order theory.

Talha & Singh[17] presented the theoretical formulations to explore the thermo mechanical study of FGMPs.

Thermo-bending problems of sandwich plates made of FG (FGSPs) were explored by Zenkour and Alghamdi [18] assuming that the sandwich plate faces are isotropic. Mechab et al. [19] analyzed flexural behavior of FGPs.

Carrera et al. [20] examined the single-layered and multilayered FG plates and shells. Daouadji et al. [21] investigated static behavior of FG plates. Neves et al. [22] analyzed FGM plates using for the static analysis.

Zenkour [23] investigated the exponentially graded plates for static problems under transverse load using both 2-D plate theory using trigonometric function (TPT) and three dimensional solutions. Mantari and Soares [24-25] explored static behaviour of exponentially graded plates (EGPs). Neves et al. [26] derived a HSDT to the static and eigen problems of FGPs.

Praveen & Reddy [27], investigated the transient analysis, based on nonlinear condition of FGPs under thermal loading using FEM.

The bending behaviour of temperature dependent FGPs resting on an elastic foundation under to thermomechanical load was investigated by Attia et al.[28]. A simple and refined nth order SDPT was developed to investigate the mechanical &

thermal buckling behaviour of FGPs. [29]. El-Haina et al.[31] Presented analytical approach to examine the thermal buckling behaviour of thick FGSPs.

Menasria et al.[32] was chosen undetermined integral based displacement function for examining thermal buckling of FGSPs. Beldjelili et al.[33] studied the hygro-therm-mechanical bending behaviour of FGPs. The vibration behaviour of the nanosize FGPs considering the quasi 3D HSDT was developed by Boutaleb et al.[34].

A simple quasi-3D HSDT was developed by Boukhelif et al.[35], to investigate the fundamental frequencies of FGPs.

Bouanati et al.[36] Used an efficient quasi 3D HSDT to explore the vibration behaviour and wave propagation of triclinic/orthotropic plate. An efficient beam theory was used by Ait Atmane et al.[37] to analyse the static analysis of FGS beams with porosity considering the elastic foundations.

Benahmed et al.[38] used hyperbolic theory to explore the static behaviour of FGP resting on elastic foundation considering the thickness stretching. Karami et al.[39] presented a quasi three dimensional theory to wave dispersion behaviour for nano FGPs resting on an elastic foundation under hygrothermal environment. Zaoui et al.[40] analysed the vibration of FGPs rests on elastic foundation using quasi-three dimensional theory. Bouhadra et al [41] developed an improved HSDT considering the stretching effect in FGPs. Younsi et al.[42] examined the static behaviour of FG plates based on hyperbolic shape function considering the thickness stretching influence.

Abualnour et al.[43] explored the frequency behaviour of the FGPs with all edges are simply support.

In this paper, a novel theory is proposed and formulated to the bending response of exponentially graded plates (EGPs) subjected to thermo-mechanical loads. The physical properties varied exponentially along with thickness direction. The equation of motion are derived using the Hamilton's principle. The present results are compared with three dimensional solutions. The influence of thermal and mechanical loads, thickness ratio and aspect ratios on the bending response of EGPs are studied in detail.

The analytical formulations and solutions presented herein could provide engineers with the potential for the design and development of exponentially graded plates for advanced engineering applications.

**2. Formulation of novel theory**

The Physical dimensions of the rectangular plate with the adopted coordinate system is shown in Fig.1. The plate is composed of entirely ceramic material at the top side and graded to the bottom side ( $z=-h/2$ ) that contains entirely metallic material. The Elastic Moduli and thermal moduli of FG plate vary exponentially along the thickness using Eq. (1), and poisons ratio ( $\nu$ ) is assumed to be constant.

$$P(z) = \text{Exp} \left[ p \left( \frac{z}{h} + \frac{1}{2} \right) \right] P_b \quad (1)$$

When  $p=0$ , it represents the property at the bottom surface and  $z=+h/2$  represents the property at the top surface i.e

$$P_t = P_b \text{Exp}[p].$$

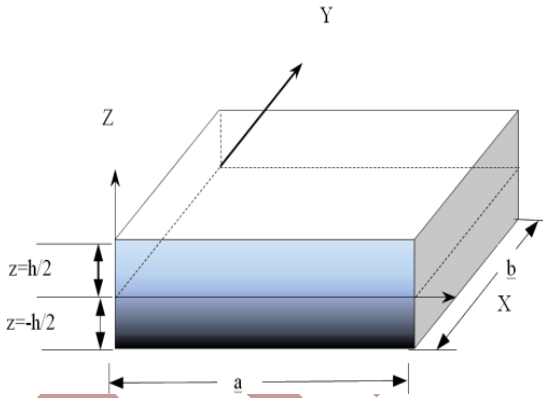


**Fig.1.** Representation of exponentially graded rectangular plate

**2.1. Displacement field**

The following is the displacement function with a is proposed for the first time.

$$u = u_0 + z[f^* \psi_x - w_{,x}] + f(z)\psi_x \quad (2a)$$

$$v = v_0 + z[f^* \psi_y - w_{,y}] + f(z)\psi_y \quad (2b)$$

$$w = w \quad (2c)$$

$$\text{Where, } f^* = \text{hav}(r/2) + \sin(r/2)/4 \quad (2d)$$

$$\text{and } f(z) = z \text{hav}(rz/h) \quad (2e)$$

The Haversine function is simply written as  $\text{hav} ( )$  in Eq. (2d-2e). The inplane displacement function is dependent on "r" and must be chosen. The optimal value of "r" is calculated after numerous computations from Eq. (8a-8f).

**2.2. Strain-Displacement Relations**

For the proposed displacement field, the strain and displacements are expressed in Eq. (2a-d).

$$\begin{Bmatrix} \varepsilon_{xx} \\ \varepsilon_{yy} \\ \varepsilon_{xy} \end{Bmatrix} = \begin{Bmatrix} u_{0,x} \\ v_{0,y} \\ u_{0,y} + v_{0,x} \end{Bmatrix} + z \begin{Bmatrix} f^* \psi_{x,x} - w_{,xx} \\ f^* \psi_{y,y} - w_{,yy} \\ f^* (\psi_{x,y} + \psi_{y,x}) - 2w_{,xy} \end{Bmatrix} + f(z) \begin{Bmatrix} \psi_{x,x} \\ \psi_{y,y} \\ \psi_{y,x} + \psi_{x,y} \end{Bmatrix} = \varepsilon + zk + f(z)k^1 \quad (3a)$$

$$\begin{Bmatrix} \gamma_{yz} \\ \gamma_{xz} \end{Bmatrix} = \begin{Bmatrix} f^* \psi_y \\ f^* \psi_x \end{Bmatrix} + f'(z) \begin{Bmatrix} \psi_y \\ \psi_x \end{Bmatrix} = \gamma + f'(z)\gamma^1 \quad (3b)$$

**2.3. Constitutive Relations**

In the present paper we consider the plane stress condition and the effect of  $\sigma_z$  is neglected. In case of FGPs the stress in plane, according to Hook's law can be written as:

$$\sigma = E(\varepsilon + zk + f(z)k^1 - \varepsilon^{th})$$

The thermal strain of the EGM plate under temperature condition is

$$\varepsilon^{th} = \alpha^T(z)\Delta T(z) \begin{bmatrix} 1 & 1 & 0 \end{bmatrix}$$

and the shear stress is

$$\tau = G(\gamma + f'(z)\gamma^1)$$

Where  $\sigma = (\sigma_{xx}, \sigma_{yy}, \tau_{xy})^t$ ,  $\tau = (\tau_{yz}, \tau_{xz})^t$

and E and G are defined as

$$E = \frac{E(z)}{1-\nu^2} \begin{bmatrix} 1 & \nu & 0 \\ \nu & 1 & 0 \\ 0 & 0 & (1-\nu)/2 \end{bmatrix}$$

$$G = \frac{E(z)}{2(1+\nu)} \begin{bmatrix} 1 & 0 \\ 0 & 1 \end{bmatrix}$$

**2.4. Equations of motion**

In analytical form, the Hamilton's principle is:

$$\int_0^t \delta U + \delta V = 0 \quad (5a)$$

$$\delta U = \int_A \left\{ \int_{-h/2}^{h/2} \left[ \begin{array}{l} \sigma_x \delta \varepsilon_{xx} + \sigma_y \delta \varepsilon_{yy} \\ + \tau_{xy} \delta \gamma_{xy} \\ + \tau_{xz} \delta \gamma_{xz} + \tau_{yz} \delta \gamma_{yz} \end{array} \right] dz \right\} dx dy \quad (5b)$$

$$\delta V = - \int q w dx dy \quad (5c)$$

By the substitution of  $\delta U$  and  $\delta V$  in the in Eq. (5a) and integrating by parts and grouping the coefficients of  $\delta u_o, \delta v_o, \delta w, \delta \psi_x,$  and  $\delta \psi_y,$  the following equations are obtained.

$$\delta u_o : N_{x,x} + N_{xy,y} = 0 \quad (6a)$$

$$\delta v_o : N_{y,y} + N_{xy,x} = 0 \quad (6b)$$

$$\delta w_o : M_{x,xx} + M_{y,yy} + 2M_{xy,xy} + q = 0 \quad (6c)$$

$$\delta \theta_x : f^* M_{x,x} + f^* M_{xy,y} + P_{x,x} + P_{xy,y} - f^* Q_{xz} - R_{xz} = 0 \quad (6d)$$

$$\delta \theta_y : f^* M_{y,y} + f^* M_{xy,x} + P_{y,y} + P_{xy,x} - f^* Q_{yz} - R_{yz} = 0 \quad (6e)$$

Where the in-plane force and transverse force moment resultants are defined as:

$$\begin{bmatrix} N_x & M_x & P_x \\ N_y & M_y & P_y \\ N_{xy} & M_{xy} & P_{xy} \end{bmatrix} = \int_{-h/2}^{h/2} \begin{bmatrix} \sigma_x \\ \sigma_y \\ \tau_{xy} \end{bmatrix} [1, z, f(z)] dz \quad (7a)$$

$$\begin{bmatrix} Q_{xz} & R_{xz} \\ Q_{yz} & R_{yz} \end{bmatrix} = \int_{-h/2}^{h/2} \begin{bmatrix} \tau_{xz} \\ \tau_{yz} \end{bmatrix} [1, f'(z)] dz \quad (7b)$$

Using Eq. (4a-c) in Eq. (7a-b), the stress resultants of exponentially graded material plates can be related to the total strains by

$$\begin{bmatrix} N \\ M \\ P \end{bmatrix} = \begin{bmatrix} A & B & E \\ B & D & F \\ E & F & H \end{bmatrix} \begin{bmatrix} \varepsilon \\ k \\ k^1 \end{bmatrix} - \begin{bmatrix} N^T \\ M^T \\ P^T \end{bmatrix} \quad (8a)$$

$$\begin{bmatrix} Q \\ R \end{bmatrix} = \begin{bmatrix} J & K \\ L & M \end{bmatrix} \begin{bmatrix} \gamma \\ \gamma^1 \end{bmatrix} \quad (8b)$$

Where  $N=[N_x, N_y, N_{xy}]^t, M= [M_x, M_y, M_{xy}]^t, P= [P_x, P_y, P_{xy}]^t, Q=[Q_{yz}, Q_{xz}]^t, R=[R_{xz}, R_{yz}]^t, NT=[NT_x, NT_y, 0]^t, M= [MT_x, MT_y, 0]^t,$  and  $P= [PT_x, PT_y, 0]^t$  (8c)

$$A = \begin{bmatrix} A_{11} & A_{12} & 0 \\ A_{12} & A_{11} & 0 \\ 0 & 0 & A_{33} \end{bmatrix}; \quad (9a)$$

$$B = \begin{bmatrix} B_{11} & B_{12} & 0 \\ B_{12} & B_{11} & 0 \\ 0 & 0 & B_{33} \end{bmatrix}; \quad (9b)$$

$$E = \begin{bmatrix} E_{11} & E_{12} & 0 \\ E_{12} & E_{11} & 0 \\ 0 & 0 & E_{33} \end{bmatrix}; \quad (9c)$$

$$D = \begin{bmatrix} D_{11} & D_{12} & 0 \\ D_{12} & D_{11} & 0 \\ 0 & 0 & D_{33} \end{bmatrix}; \quad (9d)$$

$$F = \begin{bmatrix} F_{11} & F_{12} & 0 \\ F_{12} & F_{11} & 0 \\ 0 & 0 & F_{33} \end{bmatrix}; \quad (9e)$$

$$H = \begin{bmatrix} H_{11} & H_{12} & 0 \\ H_{12} & H_{11} & 0 \\ 0 & 0 & H_{33} \end{bmatrix}; \quad (9f)$$

$$J = \begin{bmatrix} J_{11} & 0 \\ 0 & J_{11} \end{bmatrix}; \quad (9g)$$

$$K = \begin{bmatrix} K_{11} & 0 \\ 0 & K_{11} \end{bmatrix}; \quad (9h)$$

$$L = \begin{bmatrix} L_{11} & 0 \\ 0 & L_{11} \end{bmatrix}; \quad (9i)$$

$$M = \begin{bmatrix} M_{11} & 0 \\ 0 & M_{11} \end{bmatrix}; \quad (9j)$$

$$\begin{bmatrix} A_{11} & B_{11} & D_{11} & E_{11} & H_{11} & F_{11} \\ A_{12} & B_{12} & D_{12} & E_{12} & H_{12} & F_{12} \\ A_{33} & B_{33} & D_{33} & E_{33} & H_{33} & F_{33} \end{bmatrix} = \int_{-h/2}^{h/2} \frac{E(z)}{1-\nu^2} (1, z, z^2, f(z), [f(z)]^2, zf(z)) \times \begin{bmatrix} 1 \\ \nu \\ \frac{1-\nu}{2} \end{bmatrix} dz \quad (10a)$$

$$[J_{11} \quad K_{11} \quad M_{11}] = \int_{-h/2}^{h/2} \frac{E(z)}{2(1+\nu)} (1, f'(z), [f'(z)]^2) dz \quad (10b)$$

$$\begin{bmatrix} N_{xx}^T & M_{xx}^T & P_{xx}^T \\ N_{yy}^T & M_{yy}^T & P_{yy}^T \end{bmatrix} = \int_{-h/2}^{h/2} \frac{E(z)}{1-\nu^2} \begin{bmatrix} 1 & \nu \\ \nu & 1 \end{bmatrix} \alpha^T(z) \Delta T(z) \begin{bmatrix} 1 & z & f(z) \end{bmatrix} dz \quad (10c)$$

By substituting Eq. (8a-b) into Eq. (6a-e) the displacements expressed as:

$$\begin{aligned} \delta u_0 : & A_{11} u_{0,xx} + A_{12} v_{0,xy} + B_{11} (f^* \psi_{x,xx} - w_{,xxx}) \\ & + B_{12} (f^* \psi_{y,xy} - w_{,xyy}) + E_{11} \psi_{x,xx} + E_{12} \psi_{y,xy} \\ & + A_{33} (v_{0,xy} + u_{0,yy}) + B_{33} (f^* \psi_{x,yy} + f^* \psi_{y,xy} \\ & - 2w_{0,xyy}) + E_{33} (\psi_{y,xy} + \psi_{x,yy}) - N_{xx,x}^T \end{aligned} \quad (11a)$$

$$\begin{aligned} \delta v_0 : & A_{12} u_{0,xy} + A_{11} v_{0,yy} + B_{12} (f^* \psi_{x,xy} - w_{,xyy}) \\ & + B_{11} (f^* \psi_{y,yy} - w_{,yyy}) + E_{12} \psi_{x,xy} + E_{11} \psi_{y,yy} \\ & + A_{33} (v_{0,xx} + u_{0,xy}) + B_{33} (f^* \psi_{x,xy} \\ & + f^* \psi_{y,xx} - 2w_{0,xyy}) + E_{33} (\psi_{y,xx} + \psi_{x,xy}) - N_{yy,y}^T \end{aligned} \quad (11b)$$

$$\begin{aligned} \delta w : & B_{11} (u_{0,xxx} + v_{0,yyy}) + B_{12} (v_{0,xyy} + u_{0,xyy}) \\ & + D_{11} (f^* \psi_{x,xxx} + f^* \psi_{y,yyy} - w_{,yyy} - w_{,xxx}) \\ & + F_{11} (\psi_{x,xxx} + \psi_{y,yyy}) + F_{12} (\psi_{y,xyy} + \psi_{x,xyy}) \\ & + D_{12} (f^* \psi_{y,xyy} + f^* \psi_{x,xyy} - 2w_{,xyy}) \\ & + 2B_{33} (v_{0,xyy} + u_{0,xyy}) + 2D_{33} (f^* \psi_{x,xyy} \\ & + f^* \psi_{y,xyy} - 2w_{,xyy}) + F_{33} (\psi_{x,xyy} + \psi_{y,xyy}) \\ & + q - N_{xx,xx}^T - N_{yy,yy}^T \end{aligned} \quad (11c)$$

$$\begin{aligned} \delta \psi_x : & B_{11} f^* u_{0,xx} + B_{12} f^* v_{0,xy} \\ & + D_{11} (f^{*2} \psi_{x,xx} - f^* w_{,xxx}) \\ & + D_{12} (f^{*2} \psi_{y,xy} - f^* w_{,xyy}) + F_{11} f^* \psi_{x,xx} \\ & + F_{12} f^* \psi_{y,xy} + B_{33} f^* (v_{0,xy} + u_{0,yy}) \\ & + D_{33} (f^{*2} \psi_{x,yy} + f^{*2} \psi_{y,xy} - 2f^* w_{,xyy}) \\ & + F_{33} f^* (\psi_{x,yy} + \psi_{y,xy}) \\ & + E_{11} (u_{0,xx} + v_{0,xy}) + F_{11} (f^* \psi_{x,xx} - w_{,xxx}) \end{aligned}$$

$$\begin{aligned} & + F_{12} (f^* \psi_{y,xy} - w_{,xyy}) + H_{11} \psi_{x,xx} + H_{12} \psi_{y,xy} \\ & + E_{33} (u_{0,yy} + v_{0,xy}) + F_{33} (f^* \psi_{x,yy} + \psi_{y,xy} \\ & - 2w_{0,xyy}) + H_{33} (\theta_{x,yy} + \theta_{y,xy}) \\ & - (J_{11} f^{*2} - K_{11} f^* - L_{11} f^* - M_{11}) \theta_x \\ & - f^* M_{xx,x}^T - P_{xx,x}^T \end{aligned} \quad (11d)$$

$$\begin{aligned} \delta \psi_y : & B_{12} f^* u_{0,xy} + B_{11} f^* v_{0,yy} \\ & + D_{12} (f^{*2} \psi_{x,xy} - f^* w_{,xyy}) + D_{11} (f^{*2} \psi_{y,yy} - f^* w_{,yyy}) \\ & + F_{12} f^* \psi_{x,xy} + F_{11} f^* \psi_{y,yy} + B_{33} f^* (v_{0,xx} + u_{0,xy}) \\ & + D_{33} (f^{*2} \psi_{x,xy} + f^{*2} \psi_{y,xx} - 2f^* w_{,xyy}) \\ & + F_{33} f^* (\psi_{x,xy} + \psi_{y,xx}) \\ & + E_{12} (u_{0,xy} + v_{0,yy}) + F_{12} (f^* \psi_{x,xy} - w_{,xyy}) \\ & + F_{11} (f^* \psi_{y,yy} - w_{,yyy}) + H_{12} \psi_{x,xy} + H_{11} \psi_{y,yy} \\ & + E_{33} (u_{0,xy} + v_{0,xx}) + F_{33} (f^* \psi_{x,xy} + \psi_{y,xx} - 2w_{,xyy}) \\ & + H_{33} (\psi_{x,xy} + \psi_{y,xx}) \\ & - (J_{11} f^{*2} - K_{11} f^* - L_{11} f^* - M_{11}) \psi_y \\ & - f^* M_{yy,y}^T - P_{yy,y}^T \end{aligned} \quad (11e)$$

In Eq. 3(a), (6a-e) and (7a-e) comma (,) represents the partial differentiation w. r. t to the respective coordinate subscripts.

### 3. Analysis of EGPs

The solutions of the Eq. (11a -e) for EGPs with all sides are simple support and the boundary conditions for the plate is.

$$\text{At } x=0, a; \quad N_{xx} = M_{xx} = P_{xx} = v_0 = w_0 = \theta_y = \theta_z = 0 \quad (12a)$$

$$\text{At } y=0, b; \quad N_{yy} = M_{yy} = P_{yy} = u_0 = w_0 = \theta_x = \theta_z = 0 \quad (12b)$$

The sinusoidal variation of mechanical and thermal load is chosen as:

$$q(x, y) = q \sin \alpha x \sin \beta y \quad (13a)$$

The load ( $q(x, y)$ ) is in the thickness direction and  $q$  is the intensity of the load

$$T(x, y, z) = [T_1(x, y) + \frac{z}{h}T_2(x, y)] \sin \alpha x \sin \beta y \quad (13b)$$

$$+ \frac{1}{h} [zf^* + f(z)]T_3(x, y) \sin \alpha x \sin \beta y$$

Solution expressions that totally satisfy the above conditions in Eq. (14) are:

$$u_0(x, y) = u \cos \alpha x \sin \beta y \quad (14a)$$

$$v_0(x, y, t) = v \sin \alpha x \cos \beta y \quad (14b)$$

$$w(x, y) = w \sin \alpha x \sin \beta y \quad (14c)$$

$$\psi_x(x, y) = \psi \cos \alpha x \sin \beta y \quad (14d)$$

$$\psi_y(x, y) = \zeta \sin \alpha x \cos \beta y \quad (14e)$$

Where,  $0 \leq x \leq a$ ;  $0 \leq y \leq b$ ,  $\alpha = \pi/a$  and  $\beta = \pi/b$

By substituting the Eq. (14a-e) into equations of motion given by Eq. (11a-e) and by simplifying these expressions leads to a set of 5 algebraic equations involving  $u, v, w, \psi$ , and  $\zeta$  and solved using inverse method. These algebraic expressions arranged in matrix form

$$[\text{STIFFNESS MATRIX}]_{5 \times 5} [\text{UNKNOWN}]_{5 \times 1} = [\text{FORCE MATRIX}]_{5 \times 1} \quad (15)$$

The elements of the stiffness matrix are given in the Appendix.

Unknowns of the above equations gives  $u, v, w, \psi$ , and  $\zeta$  are used to compute  $u_o, v_o, w_o, \psi_x$ , and  $\psi_y$ .

#### 4. Results and discussions

The proposed displacement field dependent on ‘ $r$ ’, and the  $r$  is calculated to provide deflections and stresses of EGPs close to the three dimensional solutions [23]. It is noticed that the present novel theory estimates the bending results with minimum error with three dimensional solutions [35] at  $r=4.21$ . The bending results of simply supported EGPs using proposed HSDT for deflections and stresses under mechanical and thermal loads are presented. These numerical results are compared with the three dimensional solutions, the well known TPT, and HSDT given by Zenkour [23] and Mantari et al. [24-25].

In the present study, the displacements and normal and shear stresses, are found at their maximum absolute values. The  $u$  and  $\tau_{xz}$  are evaluated at  $(0, b/2)$ , while  $v$  and transverse shear stress  $\tau_{yz}$  are evaluated at  $(a/2, 0)$  and  $\tau_{xy}$  is evaluated at  $(0, 0)$ .

The normal stresses  $\bar{\sigma}_{yy}$  and  $w$  is evaluated at  $(a/2, b/2)$ .

All the results are given in the non dimensional quantities as follows:

$$\bar{u}, \bar{v}, \bar{w} = \frac{10}{qa^4 + \frac{10\alpha_m T_2 a^2}{E_m h^3}} (u, v, w) \quad (16a)$$

$$\bar{\sigma}_{xx}, \bar{\sigma}_{yy} = \frac{1}{qa^2 + \frac{E_m \alpha_m T_2 a^2}{h^2}} (\sigma_{xx}, \sigma_{yy}) \quad (16b)$$

$$\bar{\tau}_{xz}, \bar{\tau}_{yz} = \frac{1}{qa + \frac{E_m \alpha_m T_2 a}{h}} (\tau_{xz}, \tau_{yz}) \quad (16c)$$

$$\bar{\tau}_{xy} = \frac{10}{qa^2 + \frac{10E_m \alpha_m T_2 a^2}{h^2}} \tau_{xy} \quad (16d)$$

The numerical results of the present HSDT are presented for various  $(b/a)$  ratios and  $p$ . Fig. 2 shows the variation of exponential function in the thickness of an EGP and varies according to the Eq. (17).

$$\text{Exp} \left[ p \left( \frac{z}{h} + \frac{1}{2} \right) \right] \quad (17)$$

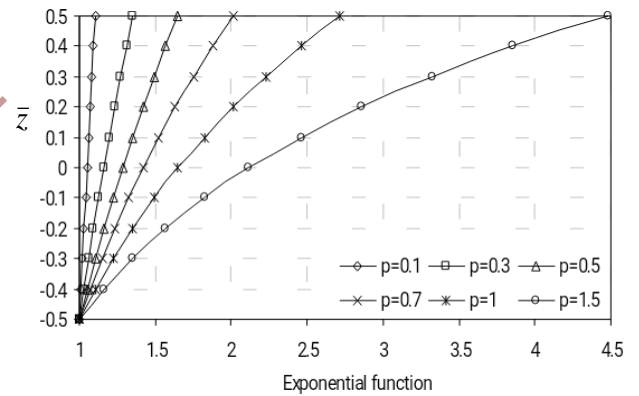


**Fig. 2.** Distribution of exponential function through the thickness of EGP.

Tables 1-3 present results of dimensionless centre deflections,  $a/h = 2, 4, 10$  respectively subjected to mechanical load.

The present results without inclusion of the thickness stretching effect,  $\epsilon_{zz} = 0$  are agreed well to three dimensional solutions and the solutions given by Mantari and Guedes Soares [25] who

considered  $\epsilon_{zz} \neq 0$ . The present theory results slightly under-estimates the 3D solutions for larger values of  $(b/a)$  and slightly over-estimates for smaller values of  $(b/a)$ . Mantari and Guedes Soares [25], also given over-estimated centre deflections in which the thickness stretching influence was not included. However, TPT [23] and HPT [23] provide under-estimated centre deflections even the thickness stretching included. Therefore, the present theory is more accurate in estimating the centre plate deflections. The dimensionless centre deflections decrease with increase of  $p$  and  $b/a$  decrease. This is due to the fact that the Young's modulus of EGM plate increases.

Fig. 3(a) shows the influence of  $a/h$  on the dimensionless centre deflection of EGP ( $p=0.5$ ).

The influence of thermal and mechanical loads is considered. The deflection is more for plate exposed to mechanical load only, while it decreases with the inclusion of thermal load (T2). The deflection behaviour of the plate is quite different and increases when the thermal load (T3) is included. Also found that the shear deformation effect decreases for  $a/h > 20$ . Fig. 3(b) shows the influence of  $b/a$  on the dimensionless centre deflection for EGP ( $p=0.5$ ). It is noted that, the centre deflection increases with increase of aspect ratio at all loading conditions, except  $q=0, T1=0, T2=1$  and  $T3=1$ . Also observed that, the inclusion of  $T2=1$  and  $T3=1$ , decrease the centre plate deflections.

**Table 1.** Comparison of  $\bar{w}$  for several EGP,  $a/h=2$

b/a	Theory	$\epsilon_{zz}$	n=0.1	n=0.3	n=0.5	n=0.7	n=1	n=1.5
6	3-D[23]		1.63774	1.48846	1.35184	1.22688	1.05929	0.82606
	<b>Present</b>	<b>0</b>	<b>1.63783</b>	<b>1.48131</b>	<b>1.33916</b>	<b>1.21009</b>	<b>1.03853</b>	<b>0.802941</b>
	Mantari et al.[25]	$\neq 0$	1.63654	1.47953	1.33644	1.20618	1.03325	0.79387
	Manteri et al.[24]	0	1.73465	1.56884	1.41822	1.28145	1.10032	0.84996
	TPT [23]	$\neq 0$	1.62939	1.47309	1.33066	1.20101	1.02823	0.79056
	HPT [23]	$\neq 0$	1.54777	1.39964	1.26493	1.14249	0.97956	0.7556
5	3-D[23]		1.60646	1.46007	1.32607	1.20349	1.03907	0.81024
	<b>Present</b>	<b>0</b>	<b>1.61009</b>	<b>1.45623</b>	<b>1.31649</b>	<b>1.18962</b>	<b>1.02097</b>	<b>0.789399</b>
	Mantari et al.[25]	$\neq 0$	1.60532	1.4513	1.31094	1.18315	1.01352	0.77867
	Manteri et al.[24]	0	1.70246	1.53972	1.39188	1.25762	1.07981	0.83401
	TPT [23]	$\neq 0$	1.59825	1.44493	1.30522	1.17804	1.00856	0.7754
	HPT [23]	$\neq 0$	1.51991	1.37444	1.24214	1.12188	0.96184	0.74184
4	3-D[23]		1.55146	1.41013	1.28074	1.16235	1.00352	0.78241
	<b>Present</b>	<b>0</b>	<b>1.5611</b>	<b>1.41193</b>	<b>1.27645</b>	<b>1.15345</b>	<b>0.989959</b>	<b>0.765472</b>
	Mantari et al.[25]	$\neq 0$	1.55042	1.40166	1.2661	1.14267	0.97884	0.75195
	Manteri et al.[24]	0	1.64584	1.48849	1.34553	1.21569	1.04374	0.80596
	TPT [23]	$\neq 0$	1.54348	1.39541	1.26048	1.13764	0.97395	0.74874
	HPT [23]	$\neq 0$	1.47089	1.33009	1.20201	1.08559	0.93065	0.71762
3	3-D[23]		1.44295	1.3116	1.19129	1.08117	0.93337	0.7275
	<b>Present</b>	<b>0</b>	<b>1.46363</b>	<b>1.32378</b>	<b>1.19677</b>	<b>1.08147</b>	<b>0.928233</b>	<b>0.717834</b>
	Mantari et al.[25]	$\neq 0$	1.4421	1.30373	1.17761	1.06279	0.91041	0.69925
	Manteri et al.[24]	0	1.53405	1.38735	1.25402	1.13291	0.97254	0.7506
	TPT [23]	$\neq 0$	1.43542	1.29771	1.17221	1.05795	0.90567	0.69615
	HPT [23]	$\neq 0$	1.37394	1.24238	1.2269	1.01386	0.86898	0.66977
2	3-D[23]		1.19445	1.08593	0.9864	0.8952	0.77266	0.60174

	<b>Present</b>	<b>0</b>	<b>1.23607</b>	<b>1.11797</b>	<b>1.01074</b>	<b>0.913395</b>	<b>0.784033</b>	<b>0.606451</b>
	Mantari et al.[25]	≠0	1.19408	1.07949	0.97503	0.8799	0.75377	0.57862
	Manteri et al.[24]	0	1.2776	1.15533	1.04413	0.94307	0.80929	0.62377
	TPT [23]	≠0	1.18798	1.07399	0.97009	0.87548	0.74936	0.57578
	HPT [23]	≠0	1.1508	1.04052	0.94012	0.84878	0.72712	0.55975
1	3-D[23]		0.57693	0.52473	0.47664	0.4324	0.37269	0.28904
	<b>Present</b>	<b>0</b>	<b>0.63847</b>	<b>0.577441</b>	<b>0.522</b>	<b>0.47166</b>	<b>0.404741</b>	<b>0.312871</b>
	Mantari et al.[25]	≠0	0.57789	0.5224	0.47179	0.42567	0.36485	0.27939
	Manteri et al.[24]	0	0.63625	0.57517	0.51948	0.46874	0.40178	0.30791
	TPT [23]	≠0	0.57308	0.51806	0.46788	0.42216	0.36117	0.27712
	HPT [23]	≠0	0.58586	0.52955	0.47814	0.43127	0.36871	0.28246

**Table 2.** Comparison of  $\bar{w}$  for several EGPs, a/h=4

b/a	Theory	$\epsilon_{zz}$	n=0.1	n=0.3	n=0.5	n=0.7	n=1	n=1.5
6	3-D[23]		1.1714	1.06218	0.96331	0.87378	0.75501	0.59193
	<b>Present</b>	<b>0</b>	<b>1.16801</b>	<b>1.05715</b>	<b>0.95706</b>	<b>0.86666</b>	<b>0.74712</b>	<b>0.58377</b>
	Mantari et al.[25]	≠0	1.17033	1.05825	0.95628	0.86359	0.74032	0.57128
	Manteri et al.[24]	0	1.19202	1.07885	0.97667	0.88437	0.76228	0.59545
	TPT [23]	≠0	1.16681	1.05509	0.95345	0.86107	0.73821	0.56969
	HPT [23]	≠0	1.00649	0.91087	0.82448	0.7464	0.64306	0.50178
5	3-D[23]		1.14589	1.03906	0.94236	0.85478	0.73859	0.57904
	<b>Present</b>	<b>0</b>	<b>1.14315</b>	<b>1.03465</b>	<b>0.93668</b>	<b>0.84821</b>	<b>0.73120</b>	<b>0.57133</b>
	Mantari et al.[25]	≠0	1.14484	1.0352	0.93545	0.84478	0.72419	0.55882
	Manteri et al.[24]	0	1.16628	1.05555	0.95557	0.86525	0.74578	0.58253
	TPT [23]	≠0	1.1414	1.0321	0.93268	0.84231	0.72212	0.55726
	HPT [23]	≠0	0.98508	0.8915	0.80694	0.7305	0.62935	0.49105
4	3-D[23]		1.10115	0.99852	0.9056	0.82145	0.70979	0.55643
	<b>Present</b>	<b>0</b>	<b>1.0995</b>	<b>0.99513</b>	<b>0.90091</b>	<b>0.81581</b>	<b>0.70326</b>	<b>0.54948</b>
	Mantari et al.[25]	≠0	1.10013	0.99477	0.89891	0.81178	0.69589	0.53696
	Manteri et al.[24]	0	1.12113	1.01469	0.91856	0.83172	0.71685	0.55987
	TPT [23]	≠0	1.09682	0.9918	0.89625	0.80941	0.6939	0.53546
	HPT [23]	≠0	0.94753	0.8575	0.77615	0.70262	0.60529	0.47222
3	3-D[23]		1.01338	0.91899	0.8335	0.75606	0.65329	0.51209
	<b>Present</b>	<b>0</b>	<b>1.01369</b>	<b>0.91746</b>	<b>0.83059</b>	<b>0.75212</b>	<b>0.64833</b>	<b>0.50652</b>
	Mantari et al.[25]	≠0	1.01243	0.91546	0.82724	0.74704	0.64037	0.49408
	Manteri et al.[24]	0	1.03254	0.9345	0.84594	0.76593	0.66008	0.51541
	TPT [23]	≠0	1.00938	0.91272	0.82479	0.74486	0.63854	0.4927
	HPT [23]	≠0	0.87379	0.79076	0.71571	0.64787	0.55806	0.43525
2	3-D[23]		0.81529	0.73946	0.67075	0.60846	0.52574	0.412
	<b>Present</b>	<b>0</b>	<b>0.819111</b>	<b>0.741343</b>	<b>0.67111</b>	<b>0.60767</b>	<b>0.52375</b>	<b>0.40908</b>



	Mantari et al.[25]	≠0	0.81448	0.73647	0.66547	0.60093	0.51508	0.39732
	Manteri et al.[24]	0	0.83246	0.75338	0.68192	0.61734	0.53188	0.41503
	TPT [23]	≠0	0.81202	0.73425	0.6635	0.59917	0.51361	0.3962
	HPT [23]	≠0	0.707	0.63979	0.57901	0.52405	0.45126	0.35169
1	3-D[23]		0.349	0.31677	0.28747	0.26083	0.22534	0.18054
	<b>Present</b>	<b>0</b>	<b>0.35522</b>	<b>0.32145</b>	<b>0.29091</b>	<b>0.26330</b>	<b>0.22674</b>	<b>0.17674</b>
	Mantari et al.[25]	≠0	0.3486	0.31519	0.28477	0.2571	0.22028	0.16972
	Manteri et al.[24]	0	0.36017	0.32589	0.29485	0.26676	0.22952	0.17854
	TPT [23]	≠0	0.34749	0.31419	0.28388	0.25631	0.21961	0.16922
	HPT [23]	≠0	0.31111	0.28146	0.25461	0.23027	0.198	0.15377

**Table 3.** Comparison of  $\bar{w}$  for several EGPs, a/h=10

b/a	Theory	$\epsilon_z$ z	n=0.1	n=0.3	n=0.5	n=0.7	n=1.0	n=1.5	n=2.0	n=2.5	n=3.0
<b>6</b>	<b>Present</b>	<b>0</b>	<b>1.035</b>	<b>0.9370</b>	<b>0.8488</b>	<b>0.7694</b>	<b>0.6645</b>	<b>0.5216</b>	<b>0.4101</b>	<b>0.3223</b>	<b>0.2530</b>
	Mantari et al.[25]	≠0	1.0354	0.9363	0.8462	0.7644	0.6558	0.5063	0.3913	0.3018	0.2324
	Manteri et al.[24]	0	1.0388	0.9405	0.852	0.7723	0.667	0.5236	0.4115	0.3235	0.2539
	TPT [23]	≠0	1.0321	0.9333	0.8436	0.7621	0.6538	0.5054	0.3901	0.3006	0.2314
<b>5</b>	<b>Present</b>	<b>0</b>	<b>1.0112</b>	<b>0.9155</b>	<b>0.8293</b>	<b>0.7517</b>	<b>0.6493</b>	<b>0.5096</b>	<b>0.4006</b>	<b>0.3149</b>	<b>0.2471</b>
	Mantari et al.[25]	≠0	1.0115	0.9147	0.8267	0.7468	0.6406	0.4952	0.3823	0.2948	0.2271
	Manteri et al.[24]	0	10.149	0.9189	0.8324	0.7545	0.6516	0.5115	0.402	0.316	0.248
	TPT [23]	≠0	1.0083	0.9118	0.8241	0.7445	0.6387	0.4938	0.381	0.2937	0.2261
<b>4</b>	<b>Present</b>	<b>0</b>	<b>0.9694</b>	<b>0.8777</b>	<b>0.7951</b>	<b>0.7207</b>	<b>0.6225</b>	<b>0.4886</b>	<b>0.3841</b>	<b>0.3019</b>	<b>0.2369</b>
	Mantari et al.[25]	≠0	0.9696	0.8768	0.7925	0.7159	0.6141	0.4747	0.3664	0.2826	0.2177
	Manteri et al.[24]	0	0.973	0.8809	0.798	0.7233	0.6247	0.4903	0.3854	0.3029	0.2377
	TPT [23]	≠0	0.9665	0.8741	0.79	0.7137	0.6123	0.4733	0.3653	0.2815	0.2167
<b>3</b>	<b>Present</b>	<b>0</b>	<b>0.8878</b>	<b>0.8037</b>	<b>0.7281</b>	<b>0.6599</b>	<b>0.5700</b>	<b>0.4474</b>	<b>0.3517</b>	<b>0.2765</b>	<b>0.21699</b>
	Mantari et al.[25]	≠0	0.8877	0.8027	0.7255	0.6554	0.5622	0.4346	0.3355	0.2587	0.1992
	Manteri et al.[24]	0	0.8909	0.8066	0.7307	0.6622	0.572	0.4489	0.3528	0.2773	0.2176
	TPT [23]	≠0	0.8849	0.8002	0.7233	0.6534	0.5605	0.4333	0.3344	0.2577	0.1983
<b>2</b>	<b>Present</b>	<b>0</b>	<b>0.7043</b>	<b>0.6376</b>	<b>0.5776</b>	<b>0.5235</b>	<b>0.4522</b>	<b>0.3549</b>	<b>0.2789</b>	<b>0.2192</b>	<b>0.1720</b>
	Mantari et al.[25]	≠0	0.7037	0.6364	0.5752	0.5196	0.4457	0.3445	0.2659	0.205	0.1579
	Manteri et al.[24]	0	0.7066	0.6397	0.5795	0.5252	0.4536	0.356	0.2797	0.2198	0.1724
	TPT [23]	≠0	0.7015	0.6344	0.5734	0.518	0.4444	0.3435	0.2651	0.2043	0.1572
<b>1</b>	<b>Present</b>	<b>0</b>	<b>0.2806</b>	<b>0.2540</b>	<b>0.2301</b>	<b>0.2085</b>	<b>0.1800</b>	<b>0.1412</b>	<b>0.1109</b>	<b>0.0871</b>	<b>0.0683</b>
	Mantari et al.[25]	≠0	0.2799	0.2531	0.2287	0.2066	0.1772	0.137	0.1057	0.0814	0.0627
	Manteri et al.[24]	0	0.2816	0.255	0.2309	0.2093	0.1807	0.1417	0.1112	0.0873	0.0684
	TPT [23]	≠0	0.279	0.2523	0.228	0.206	0.1767	0.1366	0.1053	0.0811	0.0624

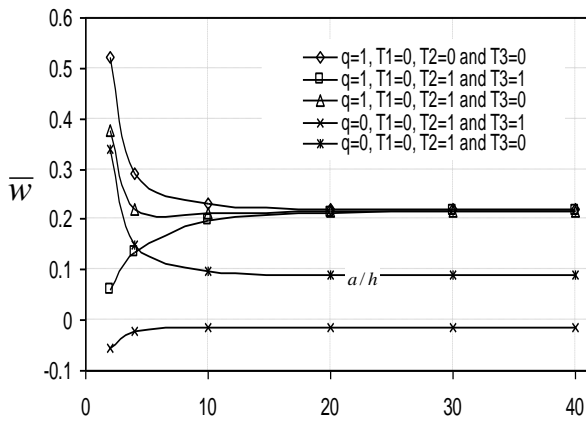


**Fig. 3(a).** Influence of thermomechanical loads on  $\bar{w}$  of square EGM Plate ( $p=0.5$ ) vs.  $a/h$

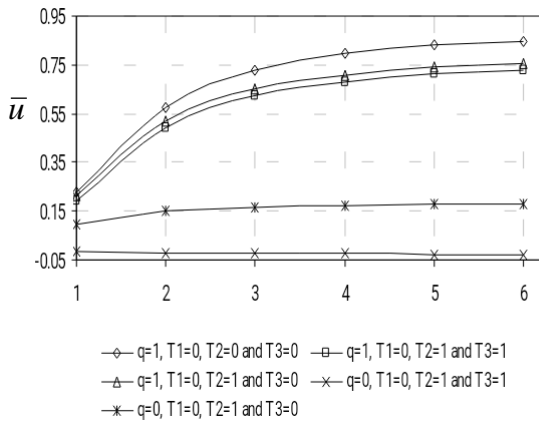


**Fig. 3(b).** Influence of thermo mechanical loads on  $\bar{u}$  of EGP ( $p=0.5$ ,  $a/h=10$ ) vs.  $a/b$

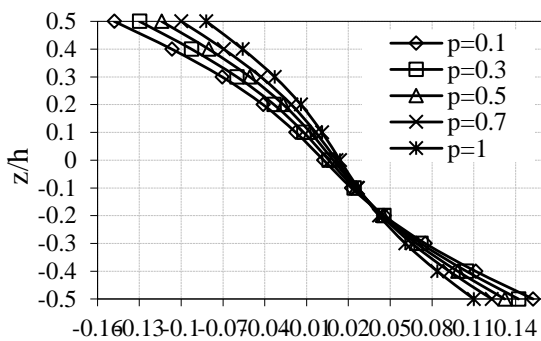


**Fig. 4(a).** Influence of  $\bar{u}$  on  $(a/h=2)$  rectangular plate ( $b/a=6$ )

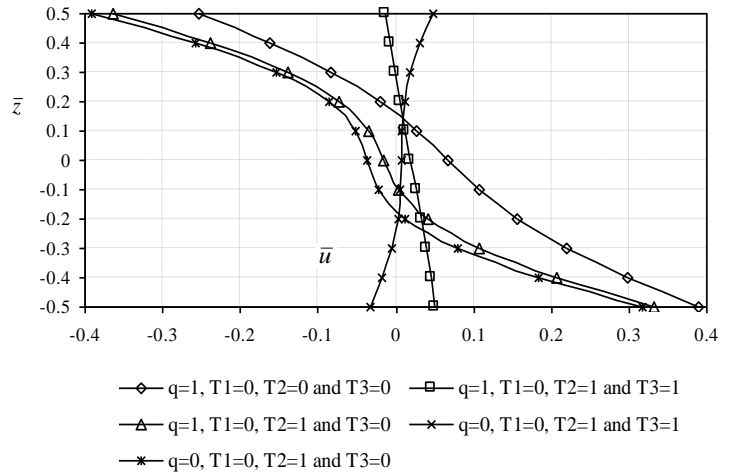


**Fig. 4(b).** Influence of  $\bar{v}$  on  $(a/h=2)$  rectangular ( $b/a=6$ ) plate

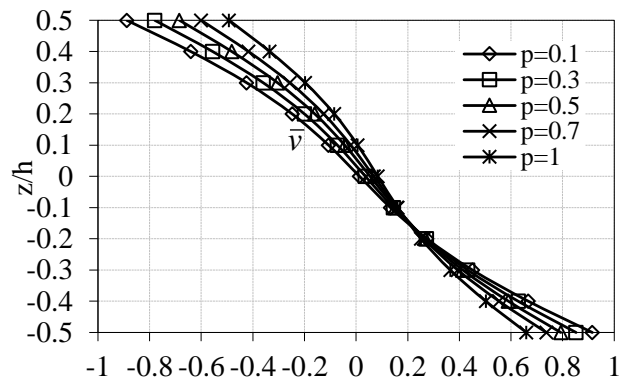


**Fig. 4(c).** Influence of thermo mechanical loads on  $\bar{u}$  of rectangular ( $b/a=2$ ) EGP ( $p=1.5$ ,  $a/h=2$ )

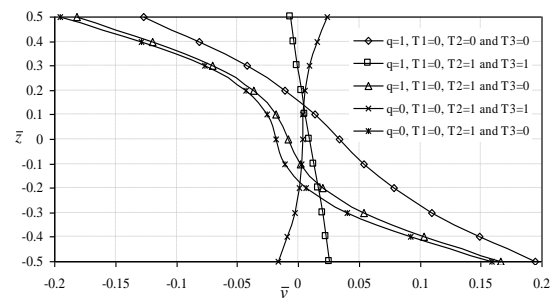


**Fig. 4(d).** Influence of thermo mechanical loads on  $\bar{v}$ , on rectangular ( $b/a=2$ ) EGP ( $p=1.5$ ,  $a/h=2$ )

The through the thickness distributions of in-plane ( $\bar{u}, \bar{v}$ ) displacements for  $p=0.1, 0.3, 0.5, 0.7$  and  $1$ , at  $a/h=2$  and  $b/a=6$  under mechanical load is shown in Fig. 4(a)-(b). The in-plane displacements increase from top side to the bottom side of the plate. At  $\bar{z} \cong -0.16$ , the in-plane displacements

\*Corresponding author

Email address: [sidhareddy\\_548@rediffmail.com](mailto:sidhareddy_548@rediffmail.com)

are independent of the exponent,  $p$ . Fig. 4 (c) -(d) show the influence of mechanical & thermal loads on in-plane displacements of the EGM plate through the thickness for  $p=1.5$ , at  $a/h=2$  and  $b/a=2$ . The in-plane displacements increase from top side of the plate to the bottom side of the plate due to the mechanical load,  $q=0$  or 1,  $T_2=1$  and  $T_3=0$ . However, the opposite can be found when,  $q=0$ ,  $T_2=T_3=1$ . The figures accentuate the pronounced influence take part by the different thermal and bending loads on the analyzed in-plane displacements.

Tables 4 to 6 present results of  $\bar{\sigma}_{yy}$  of square & rectangular EGPS,  $a/h$ : 2, 4, 10. The results for the  $\bar{\sigma}_{yy}$ , increase with the increase of  $p$ , while it decreases with  $b/a$ . The present theory results slightly under-estimating the normal stresses  $\bar{\sigma}_{yy}$ , for rectangular plates at  $a/h$ :2 & 4 and for square plates, at  $a/h$ :4, slightly over-estimating. The supremacy of the present novel theory against TPT [23], HPT [23] and Mantari et al. [24] can be notice.

The  $\bar{\sigma}_{yy}$ , are compressive at and beneath the mid-plane and tensile over the mid-plane for  $p=0.1, 0.3, 0.5, 0.7$  and 1, at  $a/h=4$  and  $b/a=2$  under mechanical load is shown in Fig. 5 (a). For the various  $p$ , chosen, the plate with  $p=1$  given the maximum tensile stress and compressive stress at the upper side and lower side of the plate, respectively. At  $\bar{z} \cong -0.275$ , the in-plane compressive stresses and at  $\bar{z} \cong 0.31$ , the in-plane tensile stresses are independent of exponent,  $p$ . Fig. 5(b) show the influence of mechanical and thermal loads on  $\bar{\sigma}_{yy}$  of EGM plate through the thickness for  $p=1.5$ , at  $a/h=2$  and  $b/a=2$ . The figure emphasis, in-plane stresses are greatly influenced by different thermal and mechanical loads.

Table 7 present results of  $\bar{\sigma}_{xx}$  of square & rectangular EGM plates at  $a/h$ :10. The results for  $\bar{\sigma}_{xx}$ , increase with increase of  $p$  & decrease of  $b/a$ . The present HSDT results are very good agreeing to the Mantari et al. [24-25]. From Fig. 6 (a) -(b) Similar inference can be drawn from the distribution  $\bar{\sigma}_{xx}$ .

Fig. 7(a) shows the distribution of in-plane shear stress,  $\bar{\tau}_{xy}$  along the thickness of the EGPs,  $a/h=2, 4, 10$ , for  $p=0.5$  and  $b/a=2$  under mechanical load. The in-plane shear stresses,  $\bar{\tau}_{xy}$ , are compressive over the middle plane of the plate and tensile at and below the middle-plane of the plate. Note that for different  $a/h$  ratios chosen, the very thick plate,  $a/h=2$  yield maximum tensile stress and minimum compressive shear stress at the bottom surface and top surface of the plate, respectively. It is important to observe that, the shear stress vary slightly, as the  $a/h$  increases through the thickness direction. At  $\bar{z} \cong \pm 0.34$ , the  $\bar{\tau}_{xy}$  are independent of the thickness of the plate. The distribution of  $\bar{\tau}_{xy}$  through the thickness direction of the EGM plate under mechanical and thermal loads is shown in Fig. 7(b). It is noticed that, the stresses are independent of the type of load at  $\bar{z} \cong 0.17$  &  $0.21$ .

The  $\bar{\sigma}_{xz}$  in different EG rectangular plates,  $p=0.1, 0.3, 0.5, 0.7, 1, 1.5, 2, 2.5, 3$ , for  $a/h=10$  is presented in Table 8. From this table it is observed that, the stress,  $\bar{\sigma}_{xz}$  decreases with both the increase of the exponent,  $p$ , and the decrease of aspect ratio,  $b/a$ . The present stress results are very close to the Manteri et al. [24-25], but TPT [23] over-estimating the stresses. Fig. 8(a) shows the distribution of shear stresses  $\bar{\sigma}_{xz}$ , through the thickness of square EGPs,  $p= \{0.1, 0.3, 0.5, 0.7, 1\}$ , for  $a/h=10$ .

**Table 4. Comparison of  $\bar{\sigma}_{yy}$  for EGPs, a/h=2**

b/a	Theory	$\epsilon_{zz}$	n=0.1	n=0.3	n=0.5	n=0.7	n=1	n=1.5
6	3-D[23]	$\neq 0$	0.29429	0.31008	0.32699	0.34508	0.37456	0.43051
	<b>Present</b>	<b>0</b>	<b>0.22421</b>	<b>0.24048</b>	<b>0.25775</b>	<b>0.27608</b>	<b>0.30568</b>	<b>0.36116</b>
	Mantari et al.[25]	$\neq 0$	0.27628	0.29544	0.31592	0.3378	0.37374	0.44163
	Manteri et al.[24]	0	0.21871	0.23447	0.25122	0.269	0.29804	0.34981
	TPT [23]	$\neq 0$	0.29119	0.31184	0.33385	0.35731	0.39547	0.46786
	HPT [23]	$\neq 0$	0.31192	0.33462	0.35873	0.38433	0.42573	0.50345
5	3-D[23]	$\neq 0$	0.29674	0.31277	0.32993	0.34829	0.37821	0.435
	<b>Present</b>	<b>0</b>	<b>0.22808</b>	<b>0.24464</b>	<b>0.26223</b>	<b>0.28089</b>	<b>0.31105</b>	<b>0.36759</b>
	Mantari et al.[25]	$\neq 0$	0.27892	0.29833	0.31905	0.34119	0.37755	0.44614
	Manteri et al.[24]	0	0.22185	0.23784	0.25484	0.27288	0.30236	0.35485
	TPT [23]	$\neq 0$	0.29353	0.31439	0.33662	0.36032	0.39884	0.47187
	HPT [23]	$\neq 0$	0.31327	0.33607	0.3603	0.38604	0.42764	0.50573
4	3-D[23]	$\neq 0$	0.30084	0.31727	0.33486	0.35368	0.38435	0.44257
	<b>Present</b>	<b>0</b>	<b>0.23473</b>	<b>0.2518</b>	<b>0.26993</b>	<b>0.28918</b>	<b>0.32029</b>	<b>0.37868</b>
	Mantari et al.[25]	$\neq 0$	0.28335	0.30317	0.32431	0.3469	0.38394	0.45373
	Manteri et al.[24]	0	0.22715	0.24354	0.26096	0.27945	0.30968	0.36337
	TPT [23]	$\neq 0$	0.29743	0.31864	0.34124	0.36533	0.40446	0.47857
	HPT [23]	$\neq 0$	0.31543	0.33842	0.36285	0.38878	0.43072	0.50943
3	3-D[23]	$\neq 0$	0.30808	0.32525	0.34362	0.36329	0.39534	0.45619
	<b>Present</b>	<b>0</b>	<b>0.24721</b>	<b>0.26524</b>	<b>0.28441</b>	<b>0.30477</b>	<b>0.33772</b>	<b>0.39965</b>
	Mantari et al.[25]	$\neq 0$	0.29122	0.31177	0.33369	0.35707	0.39537	0.46732
	Manteri et al.[24]	0	0.23675	0.25387	0.27206	0.29138	0.32297	0.37881
	TPT [23]	$\neq 0$	0.30421	0.32606	0.34933	0.3741	0.41432	0.49035
	HPT [23]	$\neq 0$	0.3189	0.3422	0.36695	0.39323	0.43572	0.51545
2	3-D[23]	$\neq 0$	0.31998	0.33849	0.35833	0.37956	0.41417	0.47989
	<b>Present</b>	<b>0</b>	<b>0.27199</b>	<b>0.29198</b>	<b>0.31327</b>	<b>0.33594</b>	<b>0.37270</b>	<b>0.44207</b>
	Mantari et al.[25]	$\neq 0$	0.30422	0.32613	0.34945	0.37427	0.41483	0.49052
	Manteri et al.[24]	0	0.25385	0.27231	0.29193	0.31276	0.3469	0.40636
	TPT [23]	$\neq 0$	0.31463	0.33758	0.362	0.38796	0.43003	0.50925
	HPT [23]	$\neq 0$	0.32223	0.34592	0.37109	0.39782	0.44102	0.52203
1	3-D[23]	$\neq 0$	0.31032	0.32923	0.34953	0.37127	0.40675	0.47405
	<b>Present</b>	<b>0</b>	<b>0.29301</b>	<b>0.31530</b>	<b>0.33915</b>	<b>0.36467</b>	<b>0.40634</b>	<b>0.48585</b>
	Mantari et al.[25]	$\neq 0$	0.29244	0.31468	0.33826	0.36325	0.40405	0.47848
	Manteri et al.[24]	0	0.25215	0.271	0.29102	0.31227	0.34773	0.40347
	TPT [23]	$\neq 0$	0.29554	0.31811	0.34208	0.3675	0.40851	0.48508
	HPT [23]	$\neq 0$	0.28882	0.31072	0.33398	0.35866	0.39852	0.47305

**Table 5. Comparison of  $\bar{\sigma}_{yy}$  for EGPs, a/h=4**

b/a	Theory	$\epsilon_{zz}$	n=0.1	n=0.3	n=0.5	n=0.7	n=1	n=1.5
6	3-D[23]	$\neq 0$	0.21814	0.23211	0.24699	0.26284	0.28857	0.33725
	<b>Present</b>	<b>0</b>	<b>0.20242</b>	<b>0.21652</b>	<b>0.23149</b>	<b>0.24740</b>	<b>0.27315</b>	<b>0.32165</b>
	Mantari et al.[25]	$\neq 0$	0.21265	0.22547	0.23934	0.2544	0.27953	0.32937
	Manteri et al.[24]	0	0.20097	0.21493	0.22976	0.24553	0.27105	0.31917
	TPT [23]	$\neq 0$	0.23686	0.25204	0.2683	0.28574	0.31441	0.3699
	HPT [23]	$\neq 0$	0.2817	0.30133	0.32219	0.34435	0.38024	0.44786
5	3-D[23]	$\neq 0$	0.2206	0.23476	0.24984	0.26591	0.29199	0.34133
	<b>Present</b>	<b>0</b>	<b>0.20529</b>	<b>0.21959</b>	<b>0.23478</b>	<b>0.25092</b>	<b>0.27705</b>	<b>0.32626</b>
	Mantari et al.[25]	$\neq 0$	0.21524	0.2283	0.24241	0.25772	0.28323	0.33373
	Manteri et al.[24]	0	0.20366	0.21781	0.23285	0.24883	0.2747	0.32346
	TPT [23]	$\neq 0$	0.23912	0.2545	0.27097	0.28863	0.31764	0.37371
	HPT [23]	$\neq 0$	0.28261	0.30231	0.32323	0.34547	0.38148	0.44934
4	3-D[23]	$\neq 0$	0.2247	0.23918	0.2546	0.27103	0.2977	0.34816
	<b>Present</b>	<b>0</b>	<b>0.21012</b>	<b>0.22476</b>	<b>0.24032</b>	<b>0.25685</b>	<b>0.28361</b>	<b>0.33402</b>
	Mantari et al.[25]	$\neq 0$	0.21957	0.23302	0.24754	0.26327	0.28943	0.34105
	Manteri et al.[24]	0	0.20818	0.22264	0.23802	0.25435	0.28081	0.33066
	TPT [23]	$\neq 0$	0.24286	0.25858	0.27539	0.29342	0.32299	0.38004
	HPT [23]	$\neq 0$	0.28399	0.30379	0.32483	0.34719	0.38338	0.45159
3	3-D[23]	$\neq 0$	0.23188	0.24692	0.26295	0.28002	0.30775	0.36021
	<b>Present</b>	<b>0</b>	<b>0.2188</b>	<b>0.23406</b>	<b>0.25027</b>	<b>0.26751</b>	<b>0.29542</b>	<b>0.34802</b>
	Mantari et al.[25]	$\neq 0$	0.22721	0.24137	0.25663	0.27312	0.30044	0.35404
	Manteri et al.[24]	0	0.21619	0.23122	0.2472	0.26417	0.29166	0.34346
	TPT [23]	$\neq 0$	0.24931	0.26563	0.28307	0.30174	0.3323	0.39106
	HPT [23]	$\neq 0$	0.28588	0.30583	0.32702	0.34954	0.38601	0.45471
2	3-D[23]	$\neq 0$	0.24314	0.25913	0.27618	0.29434	0.32385	0.37968
	<b>Present</b>	<b>0</b>	<b>0.23376</b>	<b>0.25011</b>	<b>0.26748</b>	<b>0.28596</b>	<b>0.31590</b>	<b>0.37238</b>
	Mantari et al.[25]	$\neq 0$	0.23953	0.25497	0.27154	0.28936	0.3187	0.37562
	Manteri et al.[24]	0	0.22943	0.24542	0.2624	0.28045	0.30967	0.36473
	TPT [23]	$\neq 0$	0.25878	0.27609	0.29456	0.31428	0.34644	0.40788
	HPT [23]	$\neq 0$	0.28539	0.30534	0.32655	0.34908	0.38556	0.45428
1	3-D[23]	$\neq 0$	0.22472	0.23995	0.25621	0.27356	0.30177	0.35885
	<b>Present</b>	<b>0</b>	<b>0.22527</b>	<b>0.24121</b>	<b>0.25818</b>	<b>0.27625</b>	<b>0.30557</b>	<b>0.36100</b>
	Mantari et al.[25]	$\neq 0$	0.22372	0.23907	0.25544	0.27291	0.30137	0.35555
	Manteri et al.[24]	0	0.21636	0.23157	0.24774	0.26492	0.29273	0.34508
	TPT [23]	$\neq 0$	0.23457	0.25098	0.26842	0.28698	0.31706	0.37386
	HPT [23]	$\neq 0$	0.2408	0.25783	0.27593	0.29515	0.32627	0.38482

**Table 6.** Comparison of  $\bar{\sigma}_{yy}$  for EGPs, a/h=10.

b/a	Theory	$\epsilon_{zz}$	n=0.1	n=0.3	n=0.5	n=0.7	n=1.0	n=1.5	n=2.0	n=2.5	n=3.0
<b>6</b>	<b>Present</b>	<b>0</b>	<b>0.1962</b>	<b>0.20969</b>	<b>0.2240</b>	<b>0.2392</b>	<b>0.2638</b>	<b>0.3103</b>	<b>0.3646</b>	<b>0.4279</b>	<b>0.5017</b>
	Mantari et al.[25]	≠0	0.1954	0.2065	0.2185	0.2317	0.254	0.2988	0.3552	0.4255	0.5115
	Manteri et al.[24]	0	0.198	0.2094	0.2237	0.2389	0.2635	0.31	0.3642	0.4275	0.5011
	TPT [23]	≠0	0.2223	0.236	0.2507	0.2665	0.2926	0.3435	0.4054	0.4805	0.5708
<b>5</b>	<b>Present</b>	<b>0</b>	<b>0.1988</b>	<b>0.2124</b>	<b>0.2269</b>	<b>0.2423</b>	<b>0.2673</b>	<b>0.3144</b>	<b>0.3695</b>	<b>0.4336</b>	<b>0.5083</b>
	Mantari et al.[25]	≠0	0.198	0.2093	0.2216	0.235	0.2577	0.3031	0.3602	0.4312	0.5179
	Manteri et al.[24]	0	0.1985	0.2122	0.2267	0.2421	0.267	0.314	0.369	0.4331	0.5077
	TPT [23]	≠0	0.2245	0.2385	0.2534	0.2694	0.2958	0.3473	0.4098	0.4855	0.5764
<b>4</b>	<b>Present</b>	<b>0</b>	<b>0.2031</b>	<b>0.2171</b>	<b>0.2319</b>	<b>0.2476</b>	<b>0.2732</b>	<b>0.3213</b>	<b>0.3775</b>	<b>0.4431</b>	<b>0.5195</b>
	Mantari et al.[25]	≠0	0.2023	0.214	0.2267	0.2406	0.2638	0.3104	0.3686	0.4407	0.5282
	Manteri et al.[24]	0	0.2028	0.2168	0.2316	0.2473	0.2728	0.3208	0.377	0.4424	0.5187
	TPT [23]	≠0	0.2283	0.2425	0.2578	0.2742	0.3012	0.3535	0.417	0.4937	0.5857
<b>3</b>	<b>Present</b>	<b>0</b>	<b>0.2108</b>	<b>0.2252</b>	<b>0.2406</b>	<b>0.2570</b>	<b>0.2835</b>	<b>0.3335</b>	<b>0.3918</b>	<b>0.4599</b>	<b>0.5392</b>
	Mantari et al.[25]	≠0	0.2099	0.2224	0.2358	0.2504	0.2748	0.3233	0.3835	0.4575	0.5472
	Manteri et al.[24]	0	0.2104	0.2248	0.2402	0.2565	0.2829	0.3328	0.391	0.4589	0.538
	TPT [23]	≠0	0.2347	0.2495	0.2654	0.2825	0.3104	0.3645	0.4296	0.508	0.6016
<b>2</b>	<b>Present</b>	<b>0</b>	<b>0.223</b>	<b>0.2385</b>	<b>0.2548</b>	<b>0.2722</b>	<b>0.3002</b>	<b>0.3532</b>	<b>0.4151</b>	<b>0.4873</b>	<b>0.5713</b>
	Mantari et al.[25]	≠0	0.2223	0.236	0.2507	0.2666	0.293	0.3447	0.4079	0.4846	0.5768
	Manteri et al.[24]	0	0.2225	0.2378	0.2541	0.2713	0.2993	0.3521	0.4137	0.4855	0.5692
	TPT [23]	≠0	0.2441	0.2599	0.2768	0.2949	0.3244	0.381	0.4486	0.5291	0.6246
<b>1</b>	<b>Present</b>	<b>0</b>	<b>0.2075</b>	<b>0.2218</b>	<b>0.2370</b>	<b>0.2532</b>	<b>0.2794</b>	<b>0.3288</b>	<b>0.3865</b>	<b>0.4539</b>	<b>0.5324</b>
	Mantari et al.[25]	≠0	0.2063	0.2199	0.2344	0.2499	0.2753	0.324	0.3819	0.4506	0.5317
	Manteri et al.[24]	0	0.2062	0.2204	0.2355	0.2515	0.2774	0.3264	0.3835	0.4502	0.5278
	TPT [23]	≠0	0.2196	0.2345	0.2503	0.2671	0.2944	0.346	0.4065	0.4775	0.5603

**Table 7.** Comparison of  $\bar{\sigma}_{xx}$  for EGPs, a/h=10.

b/a	Theory	$\epsilon_{zz}$	n=0.1	n=0.3	n=0.5	n=0.7	n=1.0	n=1.5	n=2.0	n=2.5	n=3.0
<b>6</b>	<b>Present</b>	<b>0</b>	<b>0.6036</b>	<b>0.6450</b>	<b>0.6891</b>	<b>0.7359</b>	<b>0.8117</b>	<b>0.9548</b>	<b>1.12181</b>	<b>1.3166</b>	<b>1.54338</b>
	Mantari et al.[25]	≠0	0.6014	0.6426	0.6864	0.7329	0.8084	0.951	1.1177	1.3124	1.9394
	Manteri et al.[24]	0	0.6029	0.6443	0.6882	0.635	0.8107	0.9536	1.1204	1.315	1.5415
	TPT [23]	≠0	0.6271	0.6707	0.717	0.7661	0.8452	0.9935	1.1651	1.3637	1.5935
<b>5</b>	<b>Present</b>	<b>0</b>	<b>0.5917</b>	<b>0.6323</b>	<b>0.6755</b>	<b>0.7214</b>	<b>0.7958</b>	<b>0.9360</b>	<b>1.0998</b>	<b>1.2908</b>	<b>1.5131</b>
	Mantari et al.[25]	≠0	0.5895	0.6299	0.6727	0.7184	0.7923	0.9321	1.0955	1.2865	1.5091
	Manteri et al.[24]	0	0.591	0.6315	0.6746	0.7205	0.7949	0.9347	1.0982	1.289	1.5111
	TPT [23]	≠0	0.6149	0.6577	0.7031	0.7512	0.8287	0.7941	1.1424	1.3372	1.5626
<b>4</b>	<b>Present</b>	<b>0</b>	<b>0.5709</b>	<b>0.6101</b>	<b>0.6518</b>	<b>0.6960</b>	<b>0.7678</b>	<b>0.9031</b>	<b>1.0611</b>	<b>1.2455</b>	<b>1.4600</b>
	Mantari et al.[25]	≠0	0.5686	0.6075	0.6488	0.6928	0.7641	0.8989	1.0566	1.241	1.456
	Manteri et al.[24]	0	0.57	0.6092	0.6508	0.695	0.7666	0.9016	1.0594	1.2434	1.4576
	TPT [23]	≠0	0.5935	0.6348	0.6785	0.6249	0.7998	0.9401	1.1025	1.2907	1.5084

<b>3</b>	<b>Present</b>	<b>0</b>	<b>0.5298</b>	<b>0.5662</b>	<b>0.6049</b>	<b>0.6460</b>	<b>0.7126</b>	<b>0.8383</b>	<b>0.9850</b>	<b>1.1562</b>	<b>1.3554</b>
	Mantari et al.[25]	≠0	0.5275	0.5635	0.6018	0.6425	0.7085	0.8335	0.98	1.1514	1.3514
	Manteri et al.[24]	0	0.5288	0.5651	0.6037	0.6447	0.7112	0.08365	0.9828	1.1536	1.3523
	TPT [23]	≠0	0.5514	0.5896	0.6302	0.6733	0.7427	0.873	1.024	1.199	1.4017
<b>2</b>	<b>Present</b>	<b>0</b>	<b>0.4363</b>	<b>0.4663</b>	<b>0.4981</b>	<b>0.5320</b>	<b>0.5869</b>	<b>0.6904</b>	<b>0.8113</b>	<b>0.9524</b>	<b>1.11679</b>
	Mantari et al.[25]	≠0	0.434	0.4634	0.4947	0.528	0.5822	0.6849	0.8056	0.9473	1.113
	Manteri et al.[24]	0	0.435	0.4649	0.4966	0.5303	0.585	0.6881	0.8085	0.949	1.1125
	TPT [23]	≠0	0.4552	0.4867	0.52	0.5554	0.6126	0.7201	0.8449	0.9898	1.158
<b>1</b>	<b>Present</b>	<b>0</b>	<b>0.2075</b>	<b>0.2218</b>	<b>0.2370</b>	<b>0.2532</b>	<b>0.2794</b>	<b>0.3288</b>	<b>0.3865</b>	<b>0.4539</b>	<b>0.5324</b>
	Mantari et al.[25]	≠0	0.2063	0.2199	0.2344	0.2499	0.2753	0.324	0.3819	0.4506	0.5317
	Manteri et al.[24]	0	0.2062	0.2204	0.2355	0.2515	0.2774	0.3264	0.3835	0.4502	0.5278
	TPT [23]	≠0	0.2196	0.2345	0.2503	0.2671	0.2944	0.346	0.4065	0.4775	0.5603

**Table 8.** Comparison of  $\bar{\sigma}_{xz}$  for EGPs, a/h=10.

b/a	Theory	$\epsilon_{zz}$	n=0.1	n=0.3	n=0.5	n=0.7	n=1.0	n=1.5	n=2.0	n=2.5	n=3.0
<b>6</b>	<b>Present</b>	<b>0</b>	<b>0.4676</b>	<b>0.4667</b>	<b>0.4650</b>	<b>0.4625</b>	<b>0.4571</b>	<b>0.4442</b>	<b>0.4267</b>	<b>0.4048</b>	<b>0.37953</b>
	Mantari et al.[25]	≠0	0.4634	0.4626	0.461	0.4586	0.4536	0.4416	0.4253	0.4065	0.3845
	Manteri et al.[24]	0	0.4633	0.4625	0.4069	0.4585	0.4536	0.4415	0.4252	0.4064	0.3842
	TPT [23]	≠0	0.4776	0.4769	0.4753	0.473	0.4681	0.4564	0.4405	0.4209	0.3981
<b>5</b>	<b>Present</b>	<b>0</b>	<b>0.4621</b>	<b>0.4613</b>	<b>0.4596</b>	<b>0.4571</b>	<b>0.4518</b>	<b>0.4390</b>	<b>0.4217</b>	<b>0.4001</b>	<b>0.37519</b>
	Mantari et al.[25]	≠0	0.4579	0.4571	0.4556	0.4532	0.4483	0.4364	0.4203	0.4017	0.38
	Manteri et al.[24]	0	0.4579	0.4571	0.4555	0.4531	0.4482	0.4363	0.4202	0.4016	0.3797
	TPT [23]	≠0	0.472	0.4713	0.4697	0.4674	0.4626	0.451	0.4353	0.4159	0.3935
<b>4</b>	<b>Present</b>	<b>0</b>	<b>0.4524</b>	<b>0.4516</b>	<b>0.4500</b>	<b>0.4475</b>	<b>0.4423</b>	<b>0.4298</b>	<b>0.4128</b>	<b>0.3918</b>	<b>0.36734</b>
	Mantari et al.[25]	≠0	0.4482	0.4475	0.4459	0.4436	0.4388	0.4271	0.4114	0.3933	0.372
	Manteri et al.[24]	0	0.4482	0.4474	0.4458	0.4435	0.4387	0.4271	0.4113	0.3931	0.3717
	TPT [23]	≠0	0.462	0.4613	0.4598	0.4575	0.4528	0.4415	0.4261	0.4071	0.3851
<b>3</b>	<b>Present</b>	<b>0</b>	<b>0.4328</b>	<b>0.4320</b>	<b>0.4304</b>	<b>0.4281</b>	<b>0.4231</b>	<b>0.4112</b>	<b>0.3949</b>	<b>0.3748</b>	<b>0.35145</b>
	Mantari et al.[25]	≠0	0.4286	0.4279	0.4264	0.4242	0.4196	0.4084	0.3934	0.3761	0.3558
	Manteri et al.[24]	0	0.4285	0.4278	0.4263	0.4241	0.4195	0.4084	0.3933	0.376	0.3555
	TPT [23]	≠0	0.4418	0.4411	0.4396	0.4375	0.433	0.4221	0.4074	0.3893	0.3686
<b>2</b>	<b>Present</b>	<b>0</b>	<b>0.3850</b>	<b>0.3843</b>	<b>0.3829</b>	<b>0.3808</b>	<b>0.3764</b>	<b>0.3658</b>	<b>0.3514</b>	<b>0.3335</b>	<b>0.3128</b>
	Mantari et al.[25]	≠0	0.381	0.3803	0.379	0.377	0.373	0.363	0.3497	0.3344	0.3165
	Manteri et al.[24]	0	0.3809	0.3803	0.3789	0.377	0.3729	0.363	0.3496	0.3343	0.3162
	TPT [23]	≠0	0.3927	0.3921	0.3908	0.3889	0.3849	0.3752	0.3621	0.346	0.3273
<b>1</b>	<b>Present</b>	<b>0</b>	<b>0.2411</b>	<b>0.2407</b>	<b>0.239</b>	<b>0.2385</b>	<b>0.2358</b>	<b>0.2292</b>	<b>0.2202</b>	<b>0.2091</b>	<b>0.19611</b>
	Mantari et al.[25]	≠0	0.238	0.2376	0.2368	0.2356	0.233	0.2268	0.2185	0.2094	0.1985
	Manteri et al.[24]	0	0.238	0.2376	0.2368	0.2356	0.233	0.2268	0.2184	0.2093	0.1983
	TPT [23]	≠0	0.2454	0.245	0.2442	0.243	0.2405	0.2344	0.2263	0.2162	0.2045

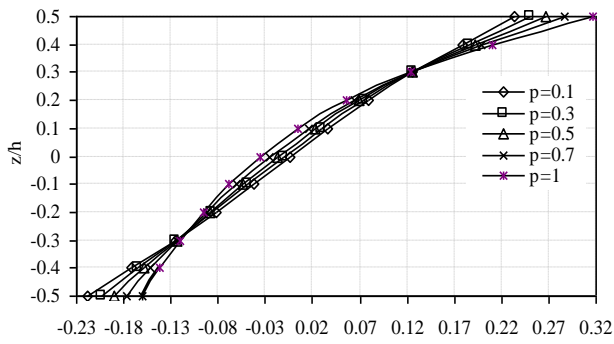


**Fig. 5(a).** Distribution of  $\bar{\sigma}_{xx}$  through the thickness of thick ( $a/h=4$ ) rectangular ( $b/a=2$ ) plate

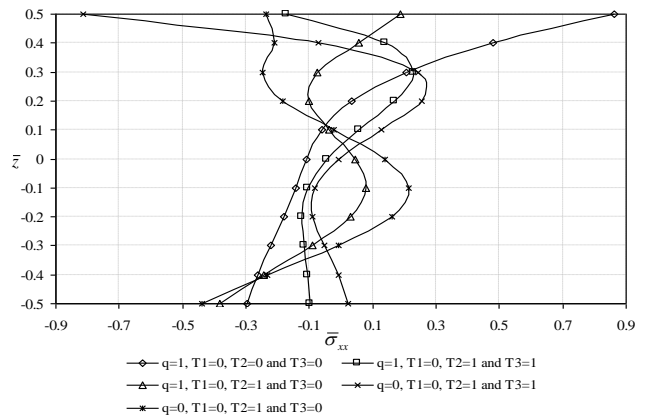


**Fig. 6(b).** Influence of thermo mechanical loads on  $\bar{\sigma}_{xx}$ , along the thickness of rectangular ( $b/a=2$ ) EGP ( $p=1.5$ ,  $a/h=2$ )

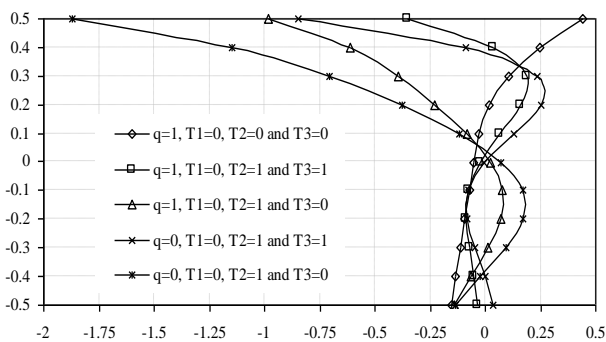


**Fig. 5(b).** Influence of thermo mechanical loads on  $\bar{\sigma}_{yy}$ , along the thickness of rectangular ( $b/a=2$ ) EGP ( $p=1.5$ ,  $a/h=2$ )

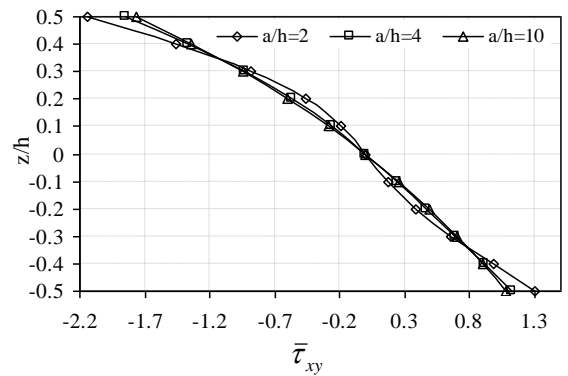


**Fig. 7(a).** Distribution of  $\bar{\tau}_{xy}$  along the thickness of rectangular ( $b/a=2$ ) EGP ( $p=0.5$ )

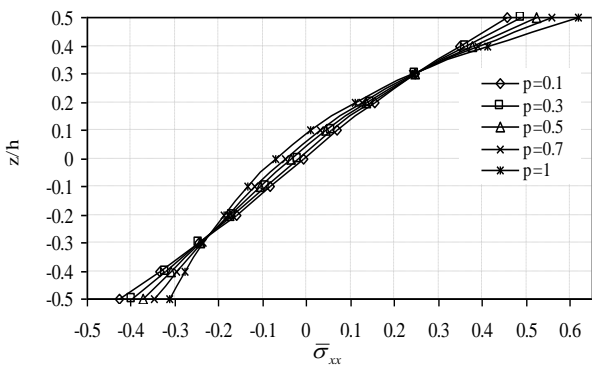


**Fig. 6(a).** Influence of  $\bar{\sigma}_{xx}$  along the thickness of thick ( $a/h=4$ ) rectangular ( $b/a=2$ ) plate

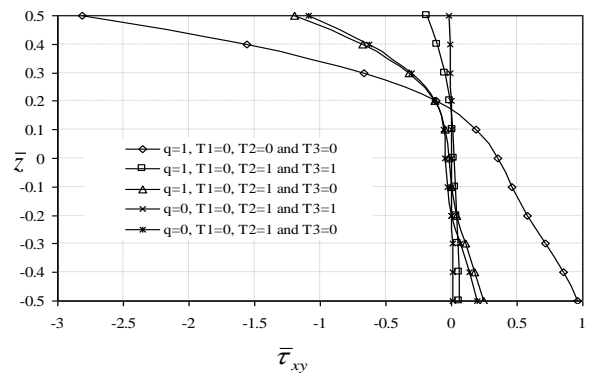


**Fig. 7(b).** Influence of thermo mechanical loads on  $\bar{\tau}_{xy}$  along the thickness of thick ( $a/h=2$ ) rectangular ( $b/a=2$ ) EGM plate ( $p=0.5$ )



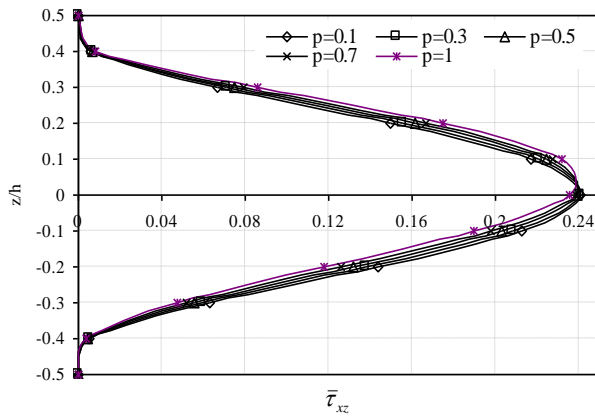


**Fig. 8(a).** Influence of  $\bar{\tau}_{xz}$  along the thickness of square EGP ( $p=0.5$ )  $a/h=10$ .

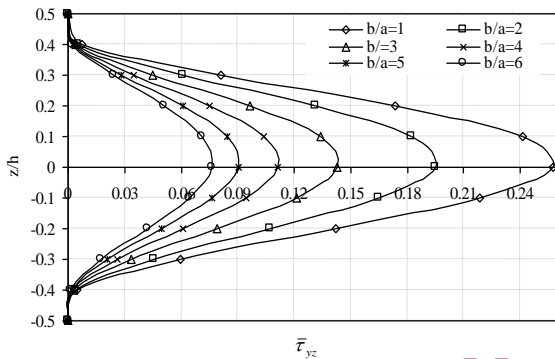


**Fig. 8(b).** Variaton of  $\bar{\tau}_{yz}$  along the thickness of ( $a/h=2$ ) EGP ( $p=0.5$ ).

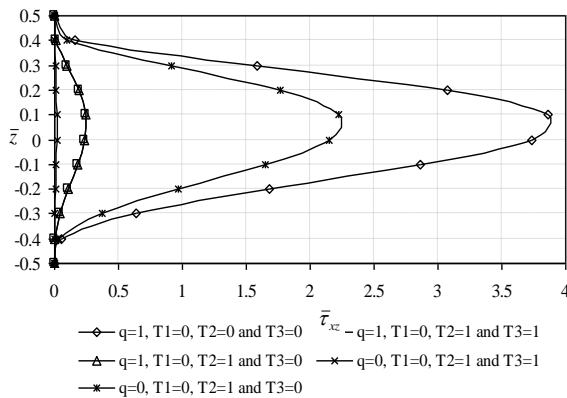


**Fig. 8(c).** Influence of mechanical & thermal loads on  $\bar{\tau}_{xz}$  along the thickness of ( $a/h=2$ ) rectangular ( $b/a=2$ ) EGP ( $p=1.5$ )

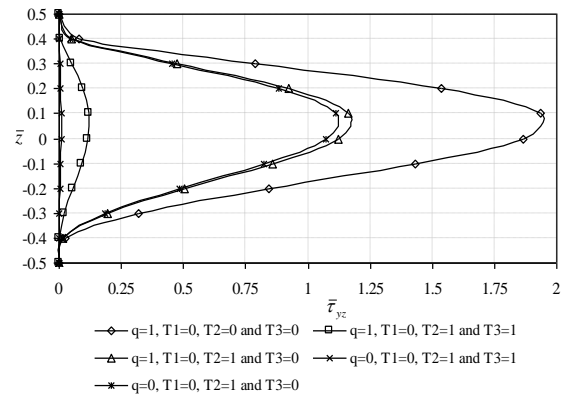


**Fig.8(d).** Influence of thermo mechanical loads on  $\bar{\tau}_{yz}$  along the thickness of thick ( $a/h=2$ ) rectangular ( $b/a=2$ ) EGP ( $p=1.5$ )

From Fig 8 (a) it can be noticed that, the stresses are maximum at the mid-plane and zero at the upper side and lower side of the plate. The stresses decrease with the increase of exponent,  $p$ , below the mid-plane and increases at and above the mid-plane. The effect of aspect ratio on stress,  $\bar{\sigma}_{yz}$  distributions along the thickness of the EGP for  $a/h$

: 2 at  $p=0.5$  is shown in Fig 8(b). The stresses are zero at the lower side and upper side of the plate and maximum at the mid-plane. The stresses decrease with the increase of  $b/a$ .

Finally, Figs. 8(c)-(d) show the distribution of  $\bar{\sigma}_{xz}$  and  $\bar{\sigma}_{yz}$ , along the thickness of the EGP, for  $a/h=2$ ,  $b/a=2$  and  $p=1.5$  under mechanical and thermal loads. From the figures, it is seen that the inclusion of thermal loads decreases the stresses. Also, the stresses are more for plate subjected to mechanical load only, whereas stresses are lesser for thermal loads only and zero at the top side and bottom side of the plate.

### 5. Conclusion

Thermomechanical behaviour of EGPs is presented based on new HSDT. The elastic and thermal moduli of the EGPs are changed exponentially along the thickness of the plate. Hamilton's principle has been used to get the equations of motion. Closedform results are obtained for EGPs under bi-sinusoidal

thermomechanical loads with all sides are simple support using Inverse method. From the numerical results, it can be inferred that the present novel theory without including stretching effect estimates the displacements and stresses of EGPs accurate with the well-known HPT [23], TPT [23] and Mantari et al. [24]. The gradients or inhomogeneities in materials play a vital role in estimating the bending behaviour of EGPs. The change of elastic moduli and thermal moduli in the thickness of the plate with exponentially can avoid interface problems and hence the stress variation is smooth. The analytical formulations and solutions presented in this paper should help in extending investigations & should provide the engineers with the potential for the design and development of exponentially graded plates for advanced engineering applications.

**Appendix**

$$\begin{aligned}
 S_{11} &= A_{11}\alpha^2 + A_{33}\beta^2 \\
 S_{12} &= (A_{12} + A_{33})\alpha\beta; \\
 S_{13} &= -B_{11}\alpha^3 - (B_{12} + 2B_{33})\alpha\beta^2; \\
 S_{14} &= (f^*B_{11} + E_{11})\alpha^2 + (f^*B_{33} + E_{33})\beta^2; \\
 S_{15} &= (f^*B_{12} + E_{12} + f^*B_{33} + E_{33})\alpha\beta; \\
 S_{21} &= (A_{21} + A_{33})\alpha\beta; \\
 S_{22} &= A_{22}\beta^2 + A_{33}\alpha^2; \\
 S_{23} &= -(B_{21} + 2B_{33})\alpha^2\beta - B_{22}\beta^3; \\
 S_{24} &= (f^*B_{21} + E_{21} + f^*B_{33} + E_{33})\alpha\beta; \\
 S_{25} &= (f^*B_{33} + E_{33})\alpha^2 + (f^*B_{22} + E_{22})\beta^2; \\
 S_{31} &= B_{11}\alpha^3 + (B_{21} + 2B_{33})\alpha\beta^2; \\
 S_{32} &= B_{22}\beta^3 + (B_{12} + 2B_{33})\alpha^2\beta; \\
 S_{33} &= -D_{11}(\alpha^4 + \beta^4) - (2D_{12} + 4D_{33})\alpha^2\beta^2; \\
 S_{34} &= (D_{11}f^* + F_{11})\alpha^3 \\
 &+ (D_{21}f^* + F_{21} + 2f^*D_{33} + F_{33})\alpha\beta^2; \\
 S_{35} &= (D_{22}f^* + F_{22})\beta^3 \\
 &+ (D_{12}f^* + F_{12} + 2f^*D_{33} + F_{33})\alpha^2\beta; \\
 S_{41} &= (B_{11}f^* + E_{11})\alpha^2 + (B_{33}f^* + E_{33})\beta^2;
 \end{aligned}$$

$$\begin{aligned}
 S_{42} &= (B_{12}f^* + f^*B_{33} + E_{12} + E_{33})\alpha\beta; \\
 S_{43} &= -(f^*D_{11} + F_{11})\alpha^3 \\
 &- (f^*D_{12} + 2f^*D_{33} + F_{12} + 2F_{33})\alpha\beta^2; \\
 S_{44} &= (f^{*2}D_{11} + 2f^*F_{11} + H_{11})\alpha^2 \\
 &+ (f^{*2}D_{33} + 2f^*F_{33} + H_{33})\beta^2 \\
 &+ J_{11}f^{*2} + K_{11}f^* + L_{11}f^* + M_{11} \\
 S_{45} &= (f^{*2}D_{12} + 2f^*F_{12} + H_{12} + H_{33} \\
 &+ f^{*2}D_{33} + 2f^*F_{33})\alpha\beta \quad ; \\
 S_{51} &= (B_{12}f^* + f^*B_{33} + E_{12} + E_{33})\alpha\beta; \\
 S_{52} &= (B_{33}f^* + E_{33})\alpha^2 + (B_{11}f^* + E_{11})\beta^2; \\
 S_{53} &= -(f^*D_{11} + F_{11})\beta^3 \\
 &- (f^*D_{12} + 2f^*D_{33} + F_{12} + 2F_{33})\alpha^2\beta; \\
 S_{54} &= (f^{*2}D_{12} + 2f^*F_{12} + H_{12} + \\
 &H_{33} + f^{*2}D_{33} + 2f^*F_{33})\alpha\beta \\
 S_{55} &= (f^{*2}D_{11} + 2f^*F_{11} + H_{11})\beta^2 \\
 &+ (f^{*2}D_{33} + 2f^*F_{33} + H_{33})\alpha^2 + J_{11}f^{*2} \\
 &+ K_{11}f^* + L_{11}f^* + M_{11} \\
 [F] &= \begin{bmatrix} -\alpha N_{xx}^T, -\beta N_{yy}^T, -q - \alpha^2 M_{xx}^T \\ -\beta^2 M_{yy}^T, \alpha(f^* M_{xx}^T + P_{xx}^T), \\ \beta(f^* M_{yy}^T + P_{yy}^T) \end{bmatrix}
 \end{aligned}$$

**References**

[1] J. N. Reddy, C. D. Chin, “Thermomechanical analysis of functionally graded cylinders and plates”. *J Therm Stresses*, Vol.21, No.6, pp. 593-626, (1998).

[2] A. M. Zenkour, “A comprehensive analysis of functionally graded sandwich plates: Part-1-Deflection and stresses”. *Int J Solids Struct*, Vol. 42, No.(18-19), pp.5224-5242, (2005).

[3] A. M. Zenkour, “A comprehensive analysis of functionally graded sandwich plates: Part-2-Buckling and free vibration”. *Int J Solids Struct*, Vol.42, No.(18-19), pp.5243-5258, (2005).

- [4] A. M. Zenkour, "Generalized shear deformation theory for bending analysis of functionally graded plates". *Appl Math Model*, Vol. 30, No.1, pp. 67-84, (2006).  
<https://doi.org/10.1016/j.apm.2005.03.009>
- [5] B. N. Pandya, T. Kant, "Higher-order shear deformable theories for flexure of sandwich plates-finite element evaluations". *Int J Solids Struct*, Vol. 24, No. 12, pp.1267-1286, (1988).
- [6] B. N. Pandya, T. Kant, "Finite element analysis of laminated composite plates using a higher order displacement model". *Compos Sci Technol*, Vol. 32, No.2, pp.137-155, (1988).
- [7] T. Kant, K. Swaminathan, "Analytical solutions for the static analysis of laminated composite and sandwich plates based on higher order refined theory". *Compos Struct*, Vol. 56, No.4, pp.329-344, (2002).
- [8] T.Kant, K.Swaminathan, "Analytical solutions for free vibration analysis of laminated composite and sandwich plates based on higher order refined theory". *Compos Struct*, Vo. 53, No.1, pp.73-85, (2001).
- [9] A. K. Garg, R. K. Khare, T. Kant, "Higher order closed form solutions for free vibration of laminated composite and sandwich shells". *J Sandw Struct Mater*, Vol. 8, No.3, pp.205-235, (2006).
- [10] M. E. Golmakani, M. Kadkhodayan, "Nonlinear bending analysis of annular FGM plates using higher order shear deformation plate theories". *Compos Struct*, Vol. 93, Pp.973-982, (2011).
- [11] H. Matsunaga, "Free vibration and stability of functionally graded plates according to a 2-D higher-order deformation theory". *Compos Struct*, Vol.82, pp.499-512 (2008).
- [12] H. Matsunaga, "Stress analysis of functionally graded plates subjected to thermal and mechanical loadings". *Compos Struct*, Vol. 87, pp.344-357, (2009).
- [13] S. Xiang, G. Kang, "A nth-order shear deformation theory for the bending analysis on the functionally graded plates". *Eur J Mech A-Solid*, Vol. 37, pp.336-343, (2013).
- [14] J. Suresh Kumar, B. Sidda Reddy, C. Eswara Reddy, K. Vijaya Kumar Reddy, "Nonlinear Thermal Analysis of Functionally Graded Plates Using Higher Order Theory". *Innovat Syst Des Eng*, Vol. 2, No. 5, pp.1-13, (2011).
- [15] B. Sidda Reddy, J. Suresh Kumar, C. Eswara Reddy, K. Vijaya Kumar Reddy, "Buckling Analysis of Functionally Graded Material Plates Using Higher Order Shear Deformation Theory", *J. Compos.*, Vol. 2013, Article ID 808764, 12 pages, (2013).
- [16] J. Suresh Kumar, B. Sidda Reddy, C. Eswara Reddy, "Nonlinear bending analysis of functionally graded plates using higher order theory". *Int. J. Eng. Sci. Technol.*, Vol. 3, No.4, pp.3010-3022, (2011).
- [17] T. Mohammad, B. N. Singh, "Thermo-mechanical deformation behavior of functionally graded rectangular plates subjected to various boundary conditions and loadings" *Int. J. Aerosp. Mech. Eng.*, Vol. 6, No.1, pp.14-25, (2012).
- [18] A. M. Zenkour, N. A. Alghamdi, "Bending analysis of functionally graded sandwich plates under the effect of mechanical and thermal loads". *Mech Adv Mate Struc*, Vol.17, No.6, pp. 419-432, (2010).
- [19] H. A. Mechab, A. Ismail, H. A. Belhadej, A. E. A. Bedia, "A two variable refined plate theory for the bending analysis of functionally graded plates". *Act Mech Sin*, Vol. 26, pp. 941-949, (2010).
- [20] E. Carrera, S. Brischetto, M. Cinefra, M Soave, "Effects of thickness stretching in functionally graded plates and shells". *Compos. B. Eng.*, Vol. 42, pp.123-133, (2011).
- [21] T. H. D. A. Henni, A. Tounsi, A. B. E. Abbes, "A New Hyperbolic Shear Deformation Theory for Bending Analysis of Functionally Graded Plates". *Model Simu Eng.*, Vol. 2012, pp. 1-10, (2012).
- [22] A.M.A. Neves, A.J.M. Ferreira, E. Carrera, M. Cinefra, C.M.C. Roque, R.M.N. Jorge, "A quasi-3d sinusoidal shear deformation theory for the static and free vibration analysis of functionally graded plates". *Compos. B. Eng.*, Vol. 43, No.711-725, (2012).
- [23] A. M. Zenkour, "Benchmark trigonometric and 3-D elasticity solutions for an exponentially graded thick rectangular plate". *Appl Math Model*, Vol. 77, pp. 197-214, (2007).

- [24] J. L. Mantari, C. Guedes Soares, "Bending analysis of thick exponentially graded plates using a new trigonometric higher order shear deformation theory". *Compos Struct* Vol. 49, pp.1991-2000, (2012).
- [25] J. L. Mantari, C. Guedes Soares, "A novel higher-order shear deformation theory with stretching effect for functionally graded plates". *Compos. B. Eng.* Vol. 45, pp.268–281, (2013).
- [26] A. M. A. Neves, A. J. M. Ferreira, E. Carrera, M. Cinefra, C. M. C. Roque, R. M. N. Jorge, C. M. M. Soares, "Static, free vibration and buckling analysis of isotropic and sandwich functionally graded plates using a quasi-3D higher-order shear deformation theory and a meshless technique". *Compos. B. Eng.*, Vol. 44 pp.657–674, (2013).
- [27] G. N. Praveen, J. N. Reddy, "Nonlinear transient thermo elastic analysis of functionally graded ceramic-metal plates". *Int J Solids Struct*, Vol. 35, pp. 4457-4476, (1998).
- [28] A. Attia, A. A. Bousahla, A. Tounsi, S.R. Mahmoud and A. S. Alwabl, "A refined four variable plate theory for thermoelastic analysis of FGM plates resting on variable elastic foundations", *Struct. Eng Mech*, Vol. 65, No. 4, pp.453-464,(2018).
- [29] A. Fahsi, A. Tounsi, H. Hebali, A. Chikh, E.A. A. Bedia and S.R. Mahmoud, "A four variable refined nth-order shear deformation theory for mechanical and thermal buckling analysis of functionally graded plates", *Geomech Eng*, Vol. 13, No. 3, pp. 385-410, (2017).
- [30] A. Chikh, A. Tounsi, H. Hebali and S. R. Mahmoud, "Thermal buckling analysis of cross-ply laminated plates using a simplified HSDT", *Smart Struct. Systems.*, Vol. 19, No. 3, pp. 289-297, (2017).
- [31] F. El-Haina, A. Bakora, A. A. Bousahla, A. Tounsi and S.R. Mahmoud, "A simple analytical approach for thermal buckling of thick functionally graded sandwich plates", *Struct Eng Mch*, Vol. 63, No. 5, pp. 585-595, (2017).
- [32] A. Menasria, A. Bouhadra, A. Tounsi, A. A. Bousahla, S.R. Mahmoud, , "A new and simple HSDT for thermal stability analysis of FG sandwich plates", *Steel Compos Struct*, Vol. 25, No. 2, pp.157-175 (2017).
- [33] Y. Beldjelili, A. Tounsi and S.R. Mahmoud, "Hygro-thermo-mechanical bending of S-FGM plates resting on variable elastic foundations using a four-variable trigonometric plate theory", *Smart Struct Syst*, Vol. 18, No. 4, pp. 755-786, (2016).
- [34] S. Boutaleb, K. H. Benrahou, A. Bakora, A. Algarni, A. A. Bousahla, A. Tounsi, and S.R. Mahmoud, "Dynamic analysis of nanosize FG rectangular plates based on simple nonlocal quasi 3D HSDT", *Advances in Nano Research*, Vol. 7, No. 3, pp.189-206, (2019).
- [35] Z. Boukhelif, M. Bouremana, F. Bourada, A. A. Bousahla, M. Bourada, A. Tounsi and M. A. Al-Osta, "A simple quasi-3D HSDT for the dynamics analysis of FG thick plate on elastic foundation", *Steel Compos Struct*, Vol. 31, No. 5, pp.503-516, (2019).
- [36] S. Bouanati, K. H. Benrahou, A. A. Hassen, A. Y. Sihame, F. Bernard, A. Tounsi and E.A. A. Bedia, "Investigation of wave propagation in anisotropic plates via quasi 3D HSDT", *Geomech Eng*, Vol. 18, No. 1, pp. 85-96 (2019).
- [37] A. A. Hassen, A. Tounsi, & F. Bernard, "Effect of thickness stretching and porosity on mechanical response of a functionally graded beams resting on elastic foundations". *Int. J. of Mech Mater Des.*, Vol. 13, No. 1, pp. 71-84, ((2017).
- [38] A. Benahmed, M. S. A. Houari, S. Benyoucef, K. Belakhdar and A. Tounsi, "A novel quasi-3D hyperbolic shear deformation theory for functionally graded thick rectangular plates on elastic foundation", *Geomech Eng*, Vol. 12, No. 1, pp. 9-34, (2017).
- [39] B. Karami, M. Janghorban, D. Shahsavari and A. Tounsi, "A size-dependent quasi-3D model for wave dispersion analysis of FG nanoplates", *Steel Compos Struct* Vol. 28, No. 1, pp. 99-110, (2018).
- [40] F. Z. Zaoui, O. Djamel & A. Tounsi, "New 2D and quasi-3D shear deformation theories for free vibration of functionally graded plates on elastic foundations", *Compos. B. Eng.*, Vol.159, pp. 231-247 ((2019).
- [41] A. Bouhadra, A. Tounsi, A. A. Bousahla, S. Benyoucef and S.R. Mahmoud, "Improved

HSDT accounting for effect of thickness stretching in advanced composite plates”, Vol. 6 *STRUCT ENG MECH*, No. 1, pp. 61-73 (2018).

- [42] A. Younsi, A. Tounsi, F. Z. Zaoui, A. A. Bousahla and S.R. Mahmoud, “Novel quasi-3D and 2D shear deformation theories for bending and free vibration analysis of FGM plates”, *Geomech Eng*, Vol. 14, No. 6, pp. 519-532, (2018).
- [43] M. Abualnour, M.S.A. Houari, A. Tounsi, E.A.A. Bedia, S.R. Mahmoud, “A novel quasi-3D trigonometric plate theory for free vibration analysis of advanced composite plates”, *Compos Struct* (2017), DOI:

EBpress